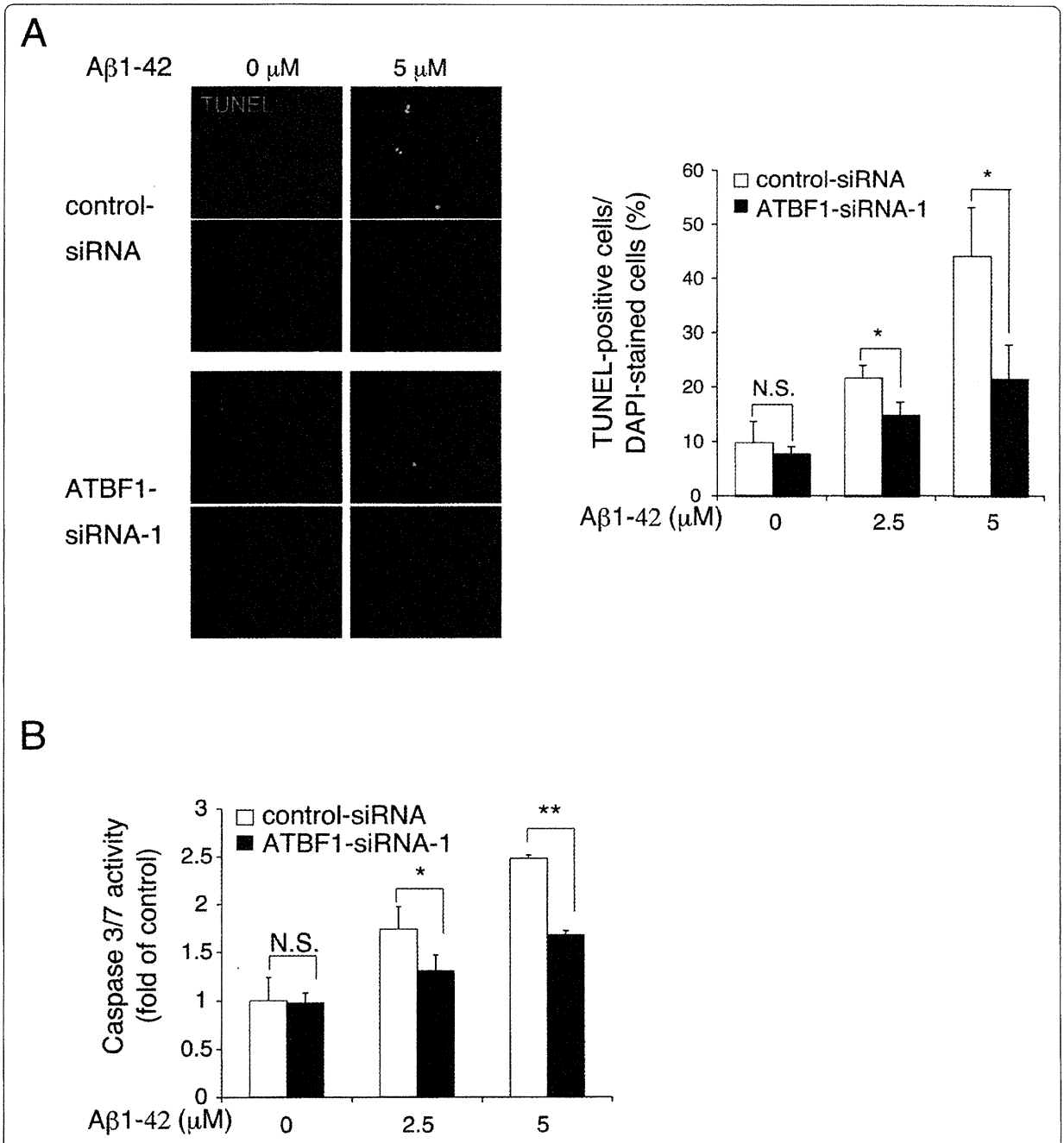

Figure 4 ATBF1 regulates apoptosis in primary cortical neurons in the presence of Aβ1-42-induced neurotoxicity. A, primary cortical neurons were seeded at a density of 1×10^6 cells/ml in poly-d-lysine-coated 24-well glass plates. Three days after plating, the cells were transfected with ATBF1 siRNA-1 or control siRNA for 48 h. After transfection, the cells were then incubated with 0, 2.5, or 10 μM Aβ1-42 for 16 h, and apoptosis was analyzed by TUNEL assay. Cell nuclei were also stained with DAPI. Left panel: Representative images showing DAPI-stained and TUNEL-positive cells. Right panel: quantification of TUNEL. TUNEL-positive neurons were counted from at least 400 neurons from five randomly selected fields in three independent experiments. B, primary cortical neurons were seeded at a density of 1×10^6 cells/ml in poly-d-lysine-coated 96-well plates. Three days after plating, cells were transfected with ATBF1 siRNA-1 or control siRNA for 48 h, and the cells were then treated with 0, 2.5, or 5 μM Aβ1-42 for 16 h. Caspase-3/7 activity was determined using a Caspase-Glo™ 3/7 assay kit. All the values are presented as the mean ± SEM of three independent experiments. *$p < 0.05$, **$p < 0.01$ *vs* control siRNA. N.S., not significant, as determined by one-way ANOVA followed by Duncan's test.

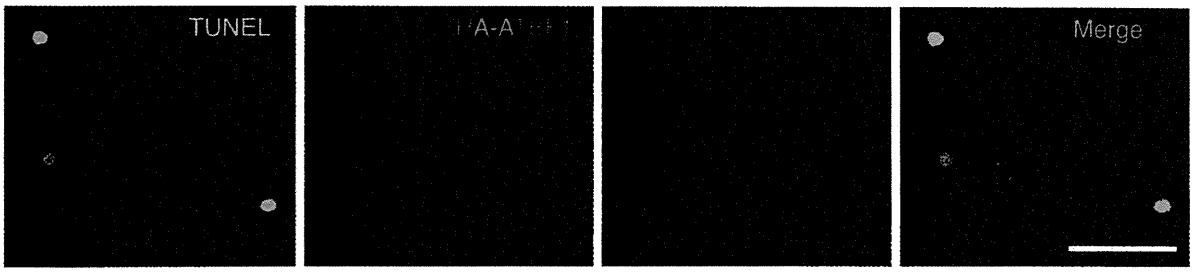

Figure 5 Overexpression of HA-tagged ATBF1 itself in primary cortical neurons did not induce apoptosis. TUNEL of primary cortical neurons transfected with HA-tagged ATBF1. The cells were transiently transfected with HA-tagged ATBF1. Twenty-four hours after transfection, TUNEL was performed, and then the cells were stained with the anti-HA antibody to detect transfected HA-ATBF1. Scale bars: 25 μm.

dead cells treated with Aβ1-42, etoposide, or homocysteine at concentration as low as 1 μM. These findings indicated that treatment with ATM inhibitors protect against Aβ1-42-, etoposide-, or homocysteine-induced neuronal death. Next, we assessed the effect of siRNA-mediated ATBF1 knockdown on Aβ1-42-induced neuronal death after treatment with caffeine or KU55933. As shown in Figure 6C and Additional file 3, there are no significant differences in the percentage of survival between ATBF1 siRNA-transfected neurons with treatment of caffeine or KU55933 and those without treatment with caffeine or KU55933. These findings indicate that ATBF1 is required for neuronal death in response to Aβ1-42 treatment, which could be dependent on ATM signaling.

ATBF1 interacted with phosphorylated ATM

It is not known whether Aβ1-42 can induce the phosphorylation of ATM in cultured cortical neurons. We therefore analyzed the effect of Aβ1-42 on the expression level of phosphorylated ATM (pATM) at Ser1981, as an indicator of ATM activation, in cultured cortical neurons. Cultured cortical neurons were treated with 10 μM Aβ1-42 for 3 h or with 1 μM etoposide for 1 h as the positive control, and pATM expression level was determined by Western blot analysis using a specific antibody to ATM at Ser1981. We found an increase in pATM levels after the treatments with Aβ1-42 and etoposide (Figure 7A). To determine whether ATBF1 interacts with pATM, coimmunoprecipitation analysis was performed. Cultured cortical neurons were treated with 10 μM Aβ1-42 for 3 h or 1 μM etoposide for 1 h, and then subjected to immunoprecipitation with anti-ATBF1 antibody-conjugated Protein G beads followed by immunoblotting with the anti-pATM antibody. As shown in Figure 7B, ATBF1 interacted with pATM after treatment with Aβ1-42 or etoposide. Our findings suggest that ATBF1 expression was enhanced by Aβ1-42 and DNA-damaging drugs (etoposide and homocysteine) and increased the expression level of ATBF1, which in turn activated ATM signaling responsible for neuronal death through the binding of ATBF1 to pATM.

ATM was required for ATBF1 to activate the p21 promoter

To determine the functional relationship between ATBF1 and ATM, we carried out p21 (Waf1/Cip1) promoter assay using ATM (+/+) and ATM (-/-) human fibroblast cells. ATM has been shown to play a role in the induction of DNA double strand breaks to arrest the cell cycle via activation of p53, and ATBF1 activates the p21 promoter in collaboration with p53 [27]. As shown in Figure 8, irradiation with X-ray increased the p21 promoter activity in ATM (+/+) cells, but not in ATM (-/-) cells, which is consistent with a previous finding that p21 expression is not changed in ATM (-/-) cells treated with the DNA-damaging drug etoposide [34]. Overexpression of ATBF1 increased the p21 promoter activity in ATM (+/+) cells, but not in ATM (-/-) cells. The combination of X-ray irradiation and overexpression of ATBF1 in ATM (+/+) cells synergistically increased p21 promoter activity. Importantly, this effect of ATBF1 on p21 promoter activity was abolished in ATM (-/-) cells. This finding indicates that ATBF1 increases p21 promoter activity in an ATM-dependent manner.

Discussion

Recently, cell-cycle-related molecules have been implicated as required components in the mechanisms underlying neuronal death in response to injury, stroke, and neurodegenerative diseases including AD [35-38] and transgenic mouse models of AD [19,20]. We have previously reported that ATBF1 is highly expressed in postmitotic neurons but not in neural progenitor cells in the developing rat brain, and that its mRNA expression level is highest in the embryonic day 12.5 (E12.5) brain [25]. Moreover, the overexpression of ATBF1 induces cell cycle arrest in mouse neuroblastoma, human prostate cancer, and human breast cancer cell

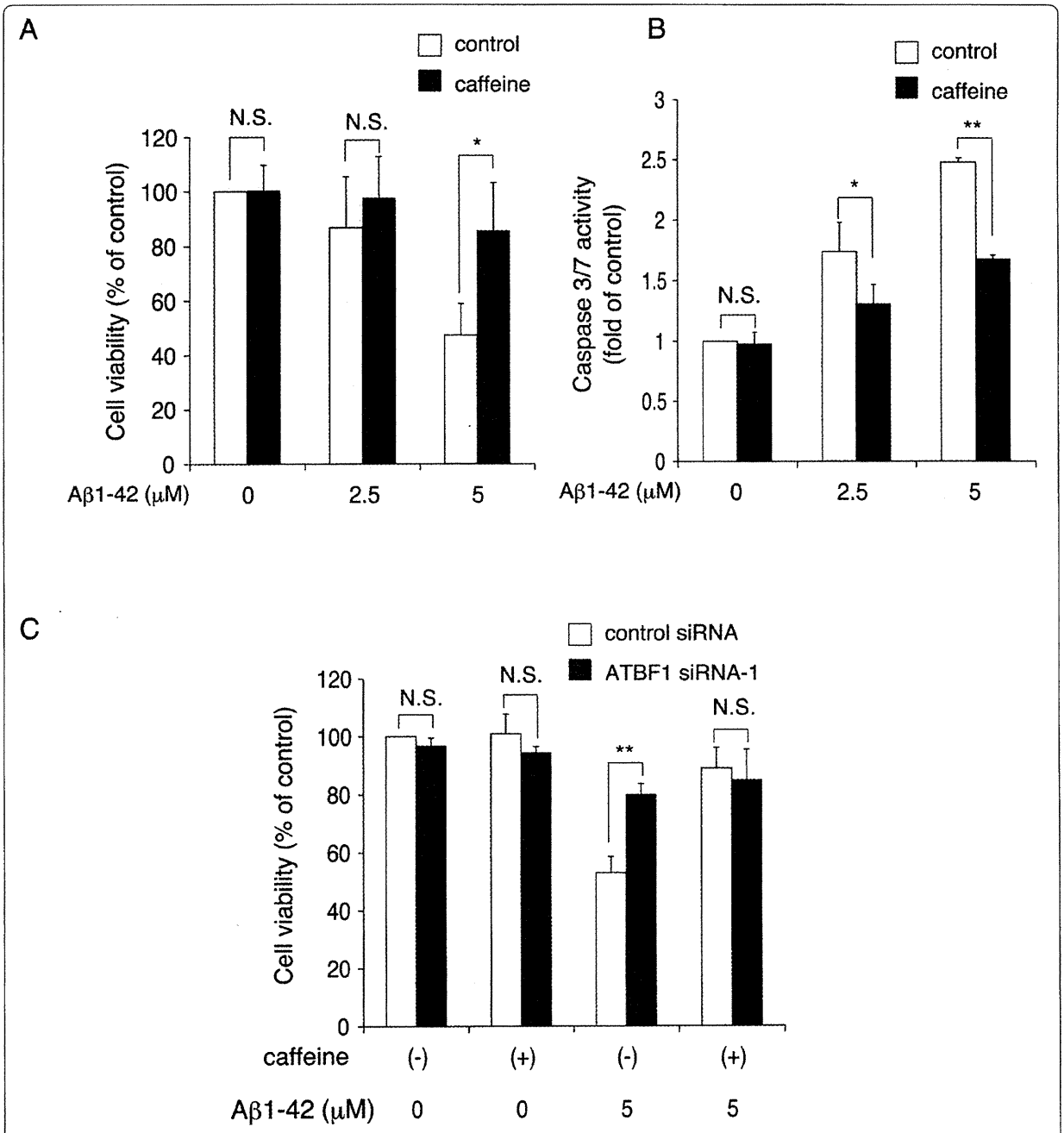

Figure 6 A and B, caffeine, an inhibitor of ATM, shows a neuroprotective effect against Aβ-induced neurotoxicity. A and B, primary cortical neurons were seeded at a density of 1×10^6 cells/ml in poly-d-lysine-coated 96-well plates. Three days after plating, cells were pretreated with 10 μM caffeine for 1 h, and subsequently treated for 16 h with 0, 2.5, or 5 μM Aβ1-42. Cell viability was determined using a CellTiter-Glo luminescent cell viability assay kit (A), and caspase-3/7 activity was determined using a Caspase-Glo™ 3/7 assay kit (B). C, after transfection as described in Fig 3B, cells were pretreated for 1 h with or without 10 μM caffeine, and then cells were further incubated with or without 5 μM Aβ1-42 for 16 h. Cell viability was determined using a CellTiter-Glo luminescent cell viability assay kit. All the values are presented as the mean ± SEM of three independent experiments. *$p < 0.05$, **$p < 0.01$ *vs* control siRNA. N.S., not significant, as determined by one-way ANOVA followed by Duncan's test.

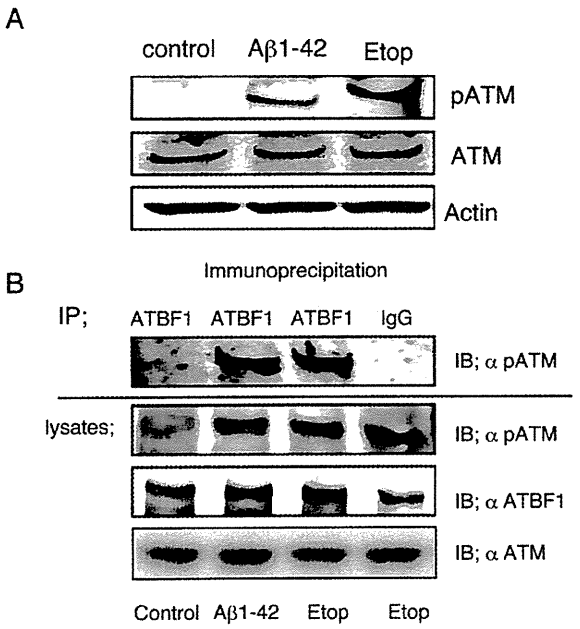

Figure 7 A, phosphorylation of ATM after treatment of primary cortical neurons with Aβ1-42 or etoposide. Primary cortical neurons were treated for 1 h with 10 μM Aβ1-42 or with 1 μM etoposide (Etop). The cells were lysed, and the protein expression levels of pATM, ATM, and actin were determined by Western blot analysis using the anti-pATM, anti-ATM, and anti-actin antibodies. B, ATBF1 interacts with pATM after treatment with Aβ1-42 or etoposide. Cultured cortical neurons were treated as described in A, cell lysates were immunoprecipitated with the anti-ATBF1 antibody. The immunoprecipitated complex was then subjected to immunoblotting with the anti-pATM at Ser1891 antibody. Typical bands representative of three independent experiments with similar results are shown.

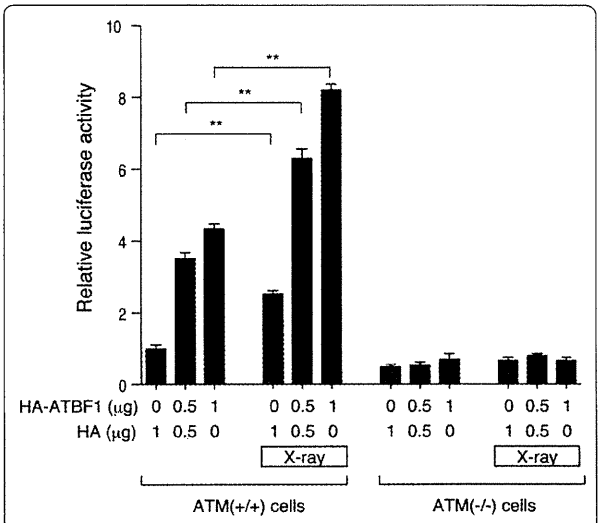

Figure 8 Effect of ATBF1 on activation of p21 promoter in X-ray-irradiated ATM (+/+) and ATM (-/-) cells. ATM (+/+) and ATM (-/-) cells were transfected with p21 promoter-luciferase, pRL-TK-luciferase (as an internal control), and an indicated dose of HA-ATBF1 vector or pCI-HA vector as a control. After 24 h, cells were irradiated with a 2.5 Gy X-ray, and then luciferase activity was measured after 12 h. All the values are presented as the mean ± SEM of three independent experiments. $^{**}p < 0.01$ *vs* not irradiated. N.S., not significant, as determined by Mann-Whitney *U*-test with Bonferroni Correction.

lines [25,28,29]. These findings suggest that ATBF1 may play critical roles in cell cycle arrest and proliferation. In the present study, we found that the ATBF1 expression level in the brains of 17-month-old wild-type mice decreased compared with that in the brains of 10-month-old wild-type mice. This finding is consistent with our previous finding that ATBF1 mRNA expression level gradually decreases with increasing age in the rat brain [25]. However, ATBF1 expression was up-regulated in the brains of 17-month-old Tg2576 mice compared with that in the brains of age-matched wild-type mice. In Tg2576 mice, diffuse plaques appear after 12 months, and their amount gradually increases with age [30]. Therefore, we considered that the increase in ATBF1 expression level was due to Aβ, and we found that the treatment with Aβ1-42 significantly increased the expression levels of ATBF1 mRNA and protein in cultured rat cortical neurons. The increase in ATBF1 expression level in the brains of 17-month-old Tg2576 mice could be triggered by the accumulation of extracellular Aβ similar to the Aβ-mediated increase in ATBF1 expression level observed in cultured cortical neurons. In addition, the reason why ATBF1 remains increased in 17-month-old Tg2576 mice could be that Aβ induces neurons to re-enter the cell cycle and ATBF1 prevents this process from occurring.

Aβ induces oxidative DNA damage. A previous study showed that the expression level of ATBF1 is increased in gastric cancer cells treated with mitomycin-C, which can induce DNA damage in many cell types [31]. This suggests that DNA damage might increase ATBF1 expression level. We, therefore, also examined whether treatment with DNA-damaging drugs, namely, etoposide and homocysteine, affects ATBF1 expression. Here, we found that these DNA-damaging drugs significantly increased the expression levels of ATBF1 mRNA and protein in cultured rat cortical neurons. These findings suggest that the up-regulated ATBF1 expression observed in our *in vivo* and *in vitro* experiments could be due to DNA damage induced by Aβ.

It has been reported that the consequences of DNA damage are the expression of cell-cycle-related proteins [22,39,40] and activation of the family of phosphatidylinositol-3 (PI3)-kinases that include the ATM protein, which is involved in the regulation of cell cycle and apoptosis by the phosphorylation of many downstream

substrates [41-43]. Therefore, one possibility is that ATM could constitute a common pathway activated in neuronal apoptosis after DNA damage. Recently, we have found that ATM induces ATBF1 expression during retinoicacid-induced neuronal differentiation of P19 cells by the activation and binding of CREB to a CRE consensus site located in the ATBF1 promoter (unpublished data). It has also been reported that the ATBF1 gene is one of the target genes of ATM that phosphorylates ATBF1 at Ser1180 [26]. These observations suggest that the activation of ATM highly correlates with the function and expression of ATBF1 as a gene regulatory factor. In this study, we observed that treatment with Aβ1-42 and etoposide rapidly posphorylates ATM at Ser 1981, and that ATBF1 interacts with pATM in cultured cortical neurons. Taken together, ATM activation induced by Aβ and DNA-damaging drugs may induce ATBF1 expression.

In this study, we also examined the effect of ATBF1 on neuronal death and apoptosis induced by Aβ1-42, etoposide, and homocysteine in cultured cortical neurons, and we found that the knockdown of ATBF1 by ATBF1 siRNA transfection significantly reduced the extent of cell death and apoptosis induced by Aβ1-42, etoposide, homocysteine. In addition, the knockdown of ATBF1 attenuated the activation of caspase-3/7. These findings suggest that the increased ATBF1 expression level may mediate apoptotic function in cultured cortical neurons against Aβ1-42-induced neurotoxicity. It has been reported that Aβ and DNA-damaging drugs induce the expression and activation of p53 which plays an important role in promoting apoptosis in cultured neurons [22,44]. Therefore, the increased ATBF1 expression level might simultaneously activate p53 to promote cell death, because ATBF1 interacts with p53 [27]. We also found in this study that ATBF1-mediated neuronal death is dependent on ATM signals because the blockage of ATM by treatment with ATM inhibitors, caffeine and KU55933, abolished ATBF1 functions in neuronal death. This finding is in agreement with our previous finding that caffeine treatment inhibits the translocalization of ATBF1 to the nucleus in P19 cells [25]. Further studies are necessary to characterize the role of ATBF1 in AD pathogenesis such as whether ATBF1 expression is altered in the AD brain.

Conclusions

In conclusion, the increase in ATBF1 expression level observed in the brain of 17-month-old Tg2576 mice compared with age-matched wild-type mice could be caused by DNA damage induced by Aβ1-42, which in turn activates the ATM signaling responsible for neuronal death, indicating that ATBF1 plays an important role in neuronal death in response to Aβ1-42, etoposide, and homocystein, and it may be a useful target in the development of drugs to suppress the neuronal death induced by Aβ1-42.

Methods

Tg2576 mice

Female Tg2576 mice, an animal model of amyloid deposition, overexpressing human APP695 with the Swedish mutation K670N/M671, were obtained from Taconic (Germantown, NY). All the experiments were performed in accordance with the Guidelines for Animal Experiments of the Animal Experimentation Committee of the National Center for Geriatrics and Gerontology.

Cell cultures

Cerebral cortical neurons were obtained from E17 Sprague-Dawley rats and cultured as described previously [45]. Briefly, embryonic brains were dissected, stripped of meninges, and minced with forceps. The minced tissue was incubated in 0.25% trypsin and 2 mg/ml DNase I in phosphate-buffered saline (PBS) at 37°C for 15 min. The fragments were then dissociated into single cells by pipetting. The dissociated cells were suspended in DMEM/F-12 medium (50:50%) containing N_2 supplements and 7.5% bovine albumin fraction V, and plated onto poly-d-lysine-coated 60 mm dishes at a density of 1×10^6/ml. These cells were used on day 4 of plating for further experiments. The immortalized fibroblast cell line AT22IJE-T was originally established from primary ataxia-telangiectasia (A-T) patient fibroblasts [46]. The cells were transfected with either the pEBS7 or pEGS7-YZ ATM vector to obtain AT22IJE-T/pEBS7 (ATM -/-) and AT22IJE-T/YZ5 (ATM +/+) cells, respectively [47]. Cells were maintained in DMEM containing 15% fetal bovine serum (FBS), 2 mM glutamine, 100 μg/ml hygromycin B, 100 U/ml penicillin, and 0.1 mg/ml streptomycin.

RNA extraction and real-time PCR

Total RNA was isolated from primary cortical neurons using an RNeasy plus mini kit (Qiagen, Valencia, CA) following the manufacturer's instructions. Reverse transcription was performed using 1 μg of total RNA using a PrimeScript RT reagent kit (Takara, Tokyo, Japan). Real-time PCR was carried out using the SYBR Premix Ex Taq system and Thermal Cycler Dice Real-Time system (Takara). The expression of the ATBF1 gene was normalized with the corresponding amount of actin mRNA using the comparative threshold cycle method following the manufacturer's protocols. Amplification was performed using the following primers (sense and antisense): ATBF1 (5'-CAAAACTTCTGCTGCCCTTC-3' and 5'-GGCTTGTCTCAAGGTGC-TTC-3') and actin (5'-CATCCGTAAAGACCTCTATGCCAAC-3' and 5'-ATGGA-GCCACCGATCCACA-3').

Aβ1–42 treatment

The synthetic Aβ1-42 peptide was purchased from Peptide Institute (Osaka, Japan), dissolved in 0.1% NH_3 to the final concentration of 1 mM, and stored at -80°C until use. To confirm the state of the Aβ1-42 peptide, we performed Western blot analysis. Briefly, a stored Aβ1-42 peptide was subjected to 16% Tris-Tricine Gel (Invitrogen) electrophoresis and transferred to polyvinylidene difluoride (PVDF) membranes (Millipore, Billerica, MA). These membranes were incubated with a primary antibody against mouse monoclonal human Aβ (6E10; Covance, Emeryville, CA). For detection, the membrane was incubated with a horseradish-peroxidase-conjugated Ig anti-mouse antibody. Immunoreaction signals were visualized with ECL™ or ECL Plus™ Western blotting detection reagent (GE Healthcare, Piscataway, NJ) and exposed to the LAS-3000 Mini Bio-imaging Analyzer System (FUJIFILM Co., Tokyo, Japan).

Western blot analysis

The cells were washed with PBS and homogenized in lysis buffer (10 mM Tris-HCl (pH 7.4), 150 mM NaCl, 1 mM EDTA, 1% Triton X-100) containing a protease inhibitor cocktail (Roche, Mannheim, Germany). The homogenates were rocked at 4°C for 30 min and centrifuged at 13,000 × *g* at 4°C for 30 min to remove cell debris. The resulting supernatant was collected and protein concentration was determined using a BCA protein assay kit (Pierce, Rockford, IL). Equal amounts of protein were subjected to 7.5% or 5-20% gradient SDS polyacrylamide gel electrophoresis, and separated products were transferred to PVDF membranes. These membranes were then blocked with 5% skim milk in 10 mM Tris-HCl (pH 7.5), 150 mM NaCl, and 0.1% Tween 20 for 1 h at room temperature or overnight at 4°C. These membranes were incubated with primary antibodies, namely, the anti-ATBF1 (AT-6) antibody (1:1000; MBL, Nagoya, Japan), anti-p53 antibody (1:1000; Cell Signaling, Cambridge, UK), anti-ATM antibody (1:1000; Gene Tex, Irvine, CA), anti-ATM kinase pS1981 antibody (1:1000; Rockland, Gilbertsville, PA), or anti-actin antibody (1:2,000; Sigma, Saint Louis, MO). The membranes were washed, and then incubated with the appropriate secondary antibody conjugated to horseradish peroxidase. Immunoreaction signals were visualized with ECL™ or ECL Plus™ Western blotting detection reagent and exposed to the LAS-3000 Mini Bio-imaging Analyzer System. Signal intensity was determined using MultiGauge software (FUJIFILM).

RNA interference

Endogenous ATBF1 was knocked down using predesigned Stealth™siRNA against ATBF1 (ATBF1 siRNA) and Stealth siRNA negative control (control siRNA) from Invitrogen (Carlsbad, CA). The ATBF1 siRNAs sequences are as follows: ATBF1-siRNA-1 sense (5'-UAC ACU GGU CAG ACC ACU GUC CUU G-3') and antisense (5'-CAA GGA CAG UGG UCU GAC CAG UGU -3'). ATBF1-siRNA-2 sense (5'- UAC ACU GGU CAG ACC ACU GUC CUU G-3') and antisense (5'-TAC ACT GGT CAG ACC ACT GTC CTT G-3'). The primary cultured neurons were transiently transfected with 50 nM ATBF1 siRNA or with control siRNA using Lipofectamine RNAiMAX (Invitrogen) in accordance with the manufacturer's instructions. The knockdown effects were examined after 48 h of incubation. The cultures were then processed for Western blot analysis, cell viability analysis and terminal deoxynucleotidyl transferase-mediated dUTP nick-end labeling (TUNEL) assay 16 h after Aβ1-42 treatment.

Cell viability analysis

Neuronal viability was evaluated by CellTiter-Glo luminescent cell viability assay (Promega, Madison, WI), which is a method to determine the number of viable cells in culture based on the quantitation of ATP present, which indicates the presence of metabolically active cells. Briefly, primary cortical neurons were seeded onto poly-d-lysine-coated 96-well plates, and incubated for 72 h. For the ATBF1 knockdown experiment, the cells were transfected with ATBF1 siRNA or with control siRNA for 48 h as described above, cells were then treated with Aβ1–42, etoposide, or homocysteine at indicated doses for 16 h. After treatment, a volume of CellTiter-Glo Reagent was added to each well equal to the volume of cell culture medium. Then, the contents were mixed for 2 min on a shaker to induce cell lysis and the plates were incubated at room temperature for 10 min in the dark. Cellular luminescence intensity was measured using a GLOMAX 96-microplate luminometer (Promega).

Plasmid constructs

The ATBF1 expression vector of an 11 kb full-length human cDNA [23] was inserted into the pCI vector (Promega) with an HA-tagged sequence at the 5'-terminus of the inserted sequence (HA-ATBF1) [25]. The 2.4 kb fragment upstream from the TATA-box of the human p21 (Waf1/Cip1) genomic fragment was subcloned into the basic luciferase reporter pGV-B vector (Toyo Ink Co., Ltd., Tokyo, Japan) [48].

TUNEL assay

Apoptosis was assessed by TUNEL using an ApopTag Fluorescein Direct In Situ Apoptosis Detection kit in accordance with the manufacturer's instructions (Chemicon, Temecula, CA). Briefly, cells were fixed with 1% paraformaldehyde in PBS for 10 min at room temperature

and permeabilized in EtOH:acetic acid (2:1) for 5 min at -20°C. Cells were then washed with PBS. Fluorescein-conjugated nucleotide and TdT enzyme were added to the cells, which were then incubated for 1 h at 37°C. Nuclei were stained with DAPI. Images were obtained using an AX70 fluorescence microscope (Olympus). The percentage of apoptotic cells was determined as the ratio of the number of DAPI-TUNEL-double-positive cells with respect to the total number of DAPI-positive cells. For the overexpression of ATBF1 in cultured cortical neurons, the neurons were transiently transfected with 0.5 μg HA-ATBF1 using FuGENE HD (Roche) in accordance with the manufacturer's instructions. Twenty-four hours after transfection, TUNEL was performed as described in above. After TUNEL, the neurons were incubated with the primary antibody against HA-tag (MBL) for 1 h at RT. The secondary antibody was Alexa-594-conjugated goat anti-rabbit IgG (Molecular Probes). Images were obtained using an AX70 fluorescence microscope (Olympus).

Caspase-3/7 activity assay

Caspase-3/7 activity was assayed using a Caspase-Glo™ 3/7 assay kit (Promega), in accordence with the manufacturer's instructions. Briefly, primary cortical neurons were seeded on 96-well plates at a density of 1×10^6 cells/ml. After 3 days, the cells were treated with Aβ1-42 or DNA-damaging drugs. Caspase-Glo™ 3/7 reagent was then added to each well, and the plates were incubated at room temperature for 1 h. Cellular luminescence was measured using a GLOMAX 96-microplate luminometer (Promega).

Immunoprecipitation

Primary cortical neurons were grown in 10 cm dishes. After reaching 50-70% confluence, the cells were treated with 10 μM Aβ1–42 or 1 μM etoposide for an indicated time. After incubation, the cells were washed twice with PBS, lysed in 1 ml of lysis buffer (10 mM Tris-HCl (pH 7.4), 150 mM NaCl, 1 mM EDTA, 1% Triton X-100, 50 mM NaF, and 100 uM sodium orthovanadate) containing protease inhibitor cocktail, and centrifuged at 13,000 × *g* at 4°C for 20 min. The resulting supernatant was immunoprecipitated overnight with a specific antibody against ATBF1 (AT-6) in the presence of protein G beads (Pierce) at 4°C. The immune complexes were washed four times with lysis buffer. The samples were subjected to 5-20% gradient SDS polyacrylamide ge electrophoresis, and separated products were transferred to a PVDF membrane and subjected to immunoblotting with a specific antibody against phosphorylated-ATM (pATM) at Ser 1981.

X-ray irradiation and p21 promoter assay

ATM (+/+) and ATM (-/-) cells were transfected with p21 promoter-luciferase, pRL-TK-luciferase (as an internal control), and an indicated dose of the HA-ATBF1 vector or pCI-HA vector as the control using Lipofectamine 2000 (Invitrogen) in accordance with manufacturer's instructions. After 24 h, the cells were irradiated with X-ray at 2.5 Gy using a Softex M-80WE X-ray generator (SOFTEX, Japan) operating at 80 kv and 10 mA for 25 min with a copper shield. Nonirradiated dells were used as control. After 12 h, luciferase activity was measured using the Dual Luciferase Reporter Assay system (Promega) in accordance with the manufacturer's instructions.

Statistical analysis

Statistical analysis was performed using a statistical package, GraphPad prism software (GraphPad Software, San Diego, CA). All values are presented as the mean ± SEM of at least three independent experiments.

Additional material

Additional file 1: Western blot analysis of Aβ1-42 peptide used in our experiments. The stored Aβ1-42 peptide was diluted with culture medium to the final concentration of 5 μM, and then 0.5 (lane 1), 1 (lane 2), or 2.5 μl (lane 3) was loaded to 16% Tris-Tricine gel and probed with the monoclonal antibody 6E10 (recognizing residues 1-17 of Aβ).

Additional file 2: Effect of another ATBF1 siRNA (ATBF1 siRNA-2) on the viability of primary cortical neurons upon treatment with Aβ1-42. A, Primary cortical neurons were transfected with ATBF1 siRNA-2 or control siRNA for 48 h. After transfection, the cells were then incubated in the presence or absence of 5 μM Aβ1-42 for 16 h. The expression levels of ATBF1 and actin were determined by Western blot analysis using the anti-ATBF1 and anti-actin antibodies. B, After transfection as described in Figure 3B, the cells were treated with or without 5 μM Aβ1-42 for 16 h. Cell viability was determined using a CellTiter-Glo luminescent cell viability assay kit and is shown as a percentage of surviving cells. All the values are presented as the mean ± SEM of three independent experiments. *$p < 0.01$ *vs* control siRNA treatment. N.S., not significant, as determined by Student's *t*-test.

Additional file 3: A, KU55933, a specific ATM inhibitor, shows a neuroprotective effect against Aβ 1-42-, etoposide-, and homocysteine-induced neurotoxicity. Primary cortical neurons were seeded at a density of 1×10^6 cells/ml in poly-d-lysine-coated 96-well plates. Three days after plating, cells were pretreated with 0, 1, 5, or 10 μM KU55933 for 1 h, and subsequently treated for 16 h with 5 μM Aβ1-42, 1 μM etoposide (Etop), or 250 μM homocysteine (Hom). Cell viability was determined using a CellTiter-Glo luminescent cell viability assay kit. B, after transfection as described in Figure 3B, cells were pretreated for 1 h with or without 1 μM KU55933, and then cells were further incubated with or without 5 μM Aβ1-42 for 16 h. Cell viability was determined using a CellTiter-Glo luminescent cell viability assay kit. All the values are presented as the mean ± SEM of three independent experiments. *$p <$ 0.001 *vs* control siRNA. N.S., not significant, as determined by one-way ANOVA followed by Duncan's test.

Abbreviations

ATBF1: AT-motif binding factor-1; Aβ: Amyloid-β peptide; AD: Alzheimer's disease; APP: Amyloid precursor protein; PS: presenilin; APOE:

apoplipoprotein E; ATM: Ataxia-telangiectasia mutated; pATM: phosphorylated ATM; PI3K: phospatidylinositol-3 kinase; TUNEL: Terminal deoxynucleotidyl transferase-mediated dUTP nick-end labeling.

Acknowledgements
We thank Eri Arata for technical assistance in Western blot analysis. We thank Makoto Nakanishi for providing the p21 (Waf1/Cip1) promoter DNA fragment. This work was supported by a Grant-in-Aid for Scientific Research (C) from the Ministry of Education, Culture, Sports, Science and Technology of Japan (CGJ) and a grant from the Japan Health Sciences Foundation for the Research on Publicly Essential Drugs and Medical Devices (MM, KHC1104) and a grant from The Research Funding for Longevity Sciences (21-A11) from National Center for Geriatrics and Gerontology (NCGG) (CGJ and MM), Japan and a Grant-in-Aid from the Japan Science and Technology Agency (YM).

Author details
[1]Department of Alzheimer's Disease Research, Research Institute, National Center for Geriatrics and Gerontology (NCGG), 35, Morioka, Obu, Aichi 474-8511, Japan. [2]Department of Molecular Neurobiology, Graduate School of Medical Sciences, Nagoya City University, Nagoya, 467-8601, Japan. [3]Queensland Institute of Medical Research and University of Queensland Centre, for Clinical Research, Brisbane 4029, Queensland, Australia.

Authors' contributions
CGJ designed this study, carried out major parts of the experiments, and drafted the manuscript. KOU prepared primary cortical neurons. YM, TH, HH, and MJK carried out the experiments. KKK provided comments on the manuscript. MM participated in the design of the study and in drafting the manuscript.
All authors have read and approved the final manuscript

Competing interests
The authors declare that they have no competing interests.

Received: 22 October 2010 Accepted: 5 July 2011 Published: 5 July 2011

References

1. Selkoe DJ: **Alzheimer's disease: genes, proteins, and therapy.** *Physiol Rev* 2001, **81**:741-766.
2. Tanzi RE, Bertram L: **Twenty years of the Alzheimer's disease amyloid hypothesis: a genetic perspective.** *Cell* 2005, **120**:545-555.
3. Goate A, Chartier-Harlin MC, Mullan M, Brown J, Crawford F, Fidani L, Giuffra L, Haynes A, Irving N, James L, *et al*: **Segregation of a missense mutation in the amyloid precursor protein gene with familial Alzheimer's disease.** *Nature* 1991, **349**:704-706.
4. Sherrington R, Rogaev EI, Liang Y, Rogaeva EA, Levesque G, Ikeda M, Chi H, Lin C, Li G, Holman K, *et al*: **Cloning of a gene bearing missense mutations in early-onset familial Alzheimer's disease.** *Nature* 1995, **375**:754-760.
5. Rogaev EI, Sherrington R, Rogaeva EA, Levesque G, Ikeda M, Liang Y, Chi H, Lin C, Holman K, Tsuda T, *et al*: **Familial Alzheimer's disease in kindreds with missense mutations in a gene on chromosome 1 related to the Alzheimer's disease type 3 gene.** *Nature* 1995, **376**:775-778.
6. Saunders AM, Strittmatter WJ, Schmechel D, George-Hyslop PH, Pericak-Vance MA, Joo SH, Rosi BL, Gusella JF, Crapper-MacLachlan DR, Alberts MJ, *et al*: **Association of apolipoprotein E allele epsilon 4 with late-onset familial and sporadic Alzheimer's disease.** *Neurology* 1993, **43**:1467-1472.
7. Frautschy SA, Baird A, Cole GM: **Effects of injected Alzheimer beta-amyloid cores in rat brain.** *Proc Natl Acad Sci USA* 1991, **88**:8362-8366.
8. Kowall NW, Beal MF, Busciglio J, Duffy LK, Yankner BA: **An in vivo model for the neurodegenerative effects of beta amyloid and protection by substance P.** *Proc Natl Acad Sci USA* 1991, **88**:7247-7251.
9. Behl C, Davis JB, Klier FG, Schubert D: **Amyloid beta peptide induces necrosis rather than apoptosis.** *Brain Res* 1994, **645**:253-264.
10. Loo DT, Copani A, Pike CJ, Whittemore ER, Walencewicz AJ, Cotman CW: **Apoptosis is induced by beta-amyloid in cultured central nervous system neurons.** *Proc Natl Acad Sci USA* 1993, **90**:7951-7955.
11. Busser J, Geldmacher DS, Herrup K: **Ectopic cell cycle proteins predict the sites of neuronal cell death in Alzheimer's disease brain.** *J Neurosci* 1998, **18**:2801-2807.
12. Liu WK, Williams RT, Hall FL, Dickson DW, Yen SH: **Detection of a Cdc2-related kinase associated with Alzheimer paired helical filaments.** *Am J Pathol* 1995, **146**:228-238.
13. McShea A, Harris PL, Webster KR, Wahl AF, Smith MA: **Abnormal expression of the cell cycle regulators P16 and CDK4 in Alzheimer's disease.** *Am J Pathol* 1997, **150**:1933-1939.
14. Vincent I, Jicha G, Rosado M, Dickson DW: **Aberrant expression of mitotic cdc2/cyclin B1 kinase in degenerating neurons of Alzheimer's disease brain.** *J Neurosci* 1997, **17**:3588-3598.
15. Copani A, Uberti D, Sortino MA, Bruno V, Nicoletti F, Memo M: **Activation of cell-cycle-associated proteins in neuronal death: a mandatory or dispensable path?** *Trends Neurosci* 2001, 25-31.
16. Ogawa O, Lee HG, Zhu X, Raina A, Harris PL, Castellani RJ, Perry G, Smith MA: **Increased p27, an essential component of cell cycle control, in Alzheimer's disease.** *Aging Cell* 2003, **2**:105-110.
17. Evans TA, Raina AK, Delacourte A, Aprelikova O, Lee HG, Zhu X, Perry G, Smith MA: **BRCA1 may modulate neuronal cell cycle re-entry in Alzheimer disease.** *Int J Med Sci* 2007, 140-145.
18. Cenini G, Sultana R, Memo M, Butterfield DA: **Effects of oxidative and nitrosative stress in brain on p53 proapoptotic protein in amnestic mild cognitive impairment and Alzheimer disease.** *Free Radic Biol Med* 2008, **45**:81-85.
19. Hsiao K, Chapman P, Nilsen S, Eckman C, Harigaya Y, Younkin S, Yang F, Cole G: **Correlative memory deficits, Abeta elevation, and amyloid plaques in transgenic mice.** *Science* 1996, **274**:99-102.
20. Yang Y, Varvel NH, Lamb BT, Herrup K: **Ectopic cell cycle events link human Alzheimer's disease and amyloid precursor protein transgenic mouse models.** *J Neurosci* 2006, **26**:775-784.
21. Lopes JP, Oliveira CR, Agostinho P: **Cdk5 acts as a mediator of neuronal cell cycle re-entry triggered by amyloid-beta and prion peptides.** *Cell Cycle* 2009, **8**:97-104.
22. Wersto RP, Cardozo-Pelaez F, Smilenov L, Chan SL, Chrest FJ, Emokpae R Jr, Gorospe M, Mattson MP: **Cell cycle activation linked to neuronal cell death initiated by DNA damage.** *Neuron* 2004, **41**:549-561.
23. Miura Y, Tam T, Ido A, Morinaga T, Miki T, Hashimoto T, Tamaoki T: **Cloning and characterization of an ATBF1 isoform that expresses in a neuronal differentiation-dependent manner.** *J Biol Chem* 1995, **270**:26840-26848.
24. Morinaga T, Yasuda H, Hashimoto T, Higashio K, Tamaoki T: **A human alpha-fetoprotein enhancer-binding protein, ATBF1, contains four homeodomains and seventeen zinc fingers.** *Mol Cell Biol* 1991, **11**:6041-6049.
25. Jung CG, Kim HJ, Kawaguchi M, Khanna KK, Hida H, Asai K, Nishino H, Miura Y: **Homeotic factor ATBF1 induces the cell cycle arrest associated with neuronal differentiation.** *Development* 2005, **132**:5137-5145.
26. Matsuoka S, Ballif BA, Smogorzewska A, McDonald ER, Hurov KE, Luo J, Bakalarski CE, Zhao Z, Solimini N, Lerenthal Y, *et al*: **ATM and ATR substrate analysis reveals extensive protein networks responsive to DNA damage.** *Science* 2007, **316**:1160-1166.
27. Miura Y, Kataoka H, Joh T, Tada T, Asai K, Nakanishi M, Okada N, Okada H: **Susceptibility to killer T cells of gastric cancer cells enhanced by Mitomycin-C involves induction of ATBF1 and activation of p21 (Waf1/Cip1) promoter.** *Microbiol Immunol* 2004, **48**:137-145.
28. Sun X, Frierson HF, Chen C, Li C, Ran Q, Otto KB, Cantarel BL, Vessella RL, Gao AC, Petros J, *et al*: **Frequent somatic mutations of the transcription factor ATBF1 in human prostate cancer.** *Nat Genet* 2005, **37**:407-412.
29. Dong XY, Sun X, Guo P, Li Q, Sasahara M, Ishii Y, Dong JT: **ATBF1 inhibits ER function by selectively competing with AIB1 for binding to ER in ER-positive breast cancer cells.** *J Biol Chem* **285(43)**:32801-9.
30. Kawarabayashi T, Younkin LH, Saido TC, Shoji M, Ashe KH, Younkin SG: **Age-dependent changes in brain, CSF, and plasma amyloid (beta) protein in the Tg2576 transgenic mouse model of Alzheimer's disease.** *J Neurosci* 2001, **21**:372-381.
31. Kamiguchi Y, Tateno H: **Radiation- and chemical-induced structural chromosome aberrations in human spermatozoa.** *Mutat Res* 2002, **504**:183-191.
32. Roth KA: **Caspases, apoptosis, and Alzheimer disease: causation, correlation, and confusion.** *J Neuropathol Exp Neurol* 2001, **60**:829-838.
33. Bryant HE, Helleday T: **Inhibition of poly (ADP-ribose) polymerase activates ATM which is required for subsequent homologous recombination repair.** *Nucleic Acids Res* 2006, **34**:1685-1691.

34. Tang D, Wu D, Hirao A, Lahti JM, Liu L, Mazza B, Kidd VJ, Mak TW, Ingram AJ: **ERK activation mediates cell cycle arrest and apoptosis after DNA damage independently of p53.** *J Biol Chem* 2002, **277**:12710-12717.
35. Greene LA, Biswas SC, Liu DX: **Cell cycle molecules and vertebrate neuron death: E2F at the hub.** *Cell Death Differ* 2004, **11**:49-60.
36. Herrup K, Neve R, Ackerman SL, Copani A: **Divide and die: cell cycle events as triggers of nerve cell death.** *J Neurosci* 2004, **24**:9232-9239.
37. Nunomura A, Moreira PI, Lee HG, Zhu X, Castellani RJ, Smith MA, Perry G: **Neuronal death and survival under oxidative stress in Alzheimer and Parkinson diseases.** *CNS Neurol Disord Drug Targets* 2007, **6**:411-423.
38. Rashidian J, Iyirhiaro GO, Park DS: **Cell cycle machinery and stroke.** *Biochim Biophys Acta* 2007, **1772**:484-493.
39. Keramaris E, Hirao A, Slack RS, Mak TW, Park DS: **Ataxia telangiectasia-mutated protein can regulate p53 and neuronal death independent of Chk2 in response to DNA damage.** *J Biol Chem* 2003, **278**:37782-37789.
40. Krantic S, Mechawar N, Reix S, Quirion R: **Molecular basis of programmed cell death involved in neurodegeneration.** *Trends Neurosci* 2005, **28**:670-676.
41. Kurz EU, Lees-Miller SP: **DNA damage-induced activation of ATM and ATM-dependent signaling pathways.** *DNA Repair (Amst)* 2004, **3**:889-900.
42. Ljungman M: **Activation of DNA damage signaling.** *Mutat Res* 2005, **577**:203-216.
43. McKinnon PJ: **Ataxia telangiectasia: new neurons and ATM.** *Trends Mol Med* 2001, **7**:233-234.
44. Uberti D, Ferrari Toninelli G, Memo M: **Involvement of DNA damage and repair systems in neurodegenerative process.** *Toxicol Lett* 2003, **139**:99-105.
45. Michikawa M, Gong JS, Fan QW, Sawamura N, Yanagisawa K: **A novel action of alzheimer's amyloid beta-protein (Abeta): oligomeric Abeta promotes lipid release.** *J Neurosci* 2001, **21**:7226-7235.
46. Ziv Y, Jaspers NG, Etkin S, Danieli T, Trakhtenbrot L, Amiel A, Ravia Y, Shiloh Y: **Cellular and molecular characteristics of an immortalized ataxia-telangiectasia (group AB) cell line.** *Cancer Res* 1989, **49**:2495-2501.
47. Ziv Y, Bar-Shira A, Pecker I, Russell P, Jorgensen TJ, Tsarfati I, Shiloh Y: **Recombinant ATM protein complements the cellular A-T phenotype.** *Oncogene* 1997, **15**:159-167.
48. Nojiri S, Joh T, Miura Y, Sakata N, Nomura T, Nakao H, Sobue S, Ohara H, Asai K, Ito M: **ATBF1 enhances the suppression of STAT3 signaling by interaction with PIAS3.** *Biochem Biophys Res Commun* 2004, **314**:97-103.

doi:10.1186/1750-1326-6-47
Cite this article as: Jung *et al.*: Beta-amyloid increases the expression level of ATBF1 responsible for death in cultured cortical neurons. *Molecular Neurodegeneration* 2011 **6**:47.

The EMBO Journal (2011) 30, 4815–4824 | © 2011 European Molecular Biology Organization | All Rights Reserved 0261-4189/11
www.embojournal.org

THE EMBO JOURNAL

Phenylpiperidine-type γ-secretase modulators target the transmembrane domain 1 of presenilin 1

Yu Ohki[1], Takuya Higo[2], Kengo Uemura[3], Naoaki Shimada[2], Satoko Osawa[1], Oksana Berezovska[3], Satoshi Yokoshima[2], Tohru Fukuyama[2], Taisuke Tomita[1,4,*] and Takeshi Iwatsubo[1,4,5,*]

[1]Department of Neuropathology and Neuroscience, Graduate School of Pharmaceutical Sciences, The University of Tokyo, Tokyo, Japan, [2]Department of Synthetic Natural Products Chemistry, Graduate School of Pharmaceutical Sciences, The University of Tokyo, Tokyo, Japan, [3]Alzheimer Research Unit, MassGeneral Institute for Neurodegenerative Disease, Massachusetts General Hospital, Charlestown, MA, USA, [4]Core Research for Evolutional Science and Technology, Japan Science and Technology Corporation, Tokyo, Japan and [5]Department of Neuropathology, Graduate School of Medicine, The University of Tokyo, Tokyo, Japan

Amyloid-β peptide ending at the 42nd residue (Aβ42) is implicated in the pathogenesis of Alzheimer's disease (AD). Small compounds that exhibit selective lowering effects on Aβ42 production are termed γ-secretase modulators (GSMs) and are deemed as promising therapeutic agents against AD, although the molecular target as well as the mechanism of action remains controversial. Here, we show that a phenylpiperidine-type compound GSM-1 directly targets the transmembrane domain (TMD) 1 of presenilin 1 (PS1) by photoaffinity labelling experiments combined with limited digestion. Binding of GSM-1 affected the structure of the initial substrate binding and the catalytic sites of the γ-secretase, thereby decreasing production of Aβ42, possibly by enhancing its conversion to Aβ38. These data indicate an allosteric action of GSM-1 by directly binding to the TMD1 of PS1, pinpointing the target structure of the phenylpiperidine-type GSMs.

The EMBO Journal (2011) **30,** 4815–4824. doi:10.1038/emboj.2011.372; Published online 14 October 2011
Subject Categories: neuroscience; molecular biology of disease
Keywords: Alzheimer; modulation; protease; secretase

Introduction

There is ample evidence supporting the notion that aggregation of amyloid-β peptides (Aβ) underlies the pathogenesis of Alzheimer's disease (AD) (reviewed by Holtzman *et al*, 2011). Aβ is a proteolytic fragment of amyloid precursor protein (APP) derived by sequential cleavages by two proteases termed β- and γ-secretases. γ-Secretase determines the C-terminal length of Aβ, which in turn impacts the aggregation property of Aβ: the C-terminally longer Aβ42 is the initially deposited and the most aggregation-prone species linked to the pathogenesis of AD (Iwatsubo *et al*, 1994). Thus, small compounds that regulate the activity of γ-secretase have been developed as disease-modifying drugs against AD (Tomita, 2009; De Strooper *et al*, 2010). However, conventional γ-secretase inhibitors (GSIs) that block the proteolytic cleavage of numerous substrate proteins in a non-specific fashion cause severe adverse effects. For example, GSIs interfere with Notch receptor signalling that is essential to development and differentiation, and is activated by the γ-secretase cleavage (Extance, 2010). The discovery that a subset of non-steroidal anti-inflammatory drugs (NSAIDs) act as a γ-secretase modulator (GSM) that selectively and directly reduces Aβ42 without affecting the total γ-secretase activity opened up a way to the safe and effective lowering of the pathogenic Aβ42 while sparing the Notch signalling (Weggen *et al*, 2001; Takahashi *et al*, 2003). Although the clinical trial of Flurizan (*R*-Flurbiprofen), an NSAID-type GSM, failed because of the low penetrance of the compound into the brain (Green *et al*, 2009), several potent GSMs with excellent brain availability are emerging, raising high hopes for the treatment of AD (Tomita, 2009; De Strooper *et al*, 2010).

γ-Secretase is an atypical intramembrane protease that comprising four integral membrane proteins, that is, presenilin (PS), nicastrin, Aph-1 and Pen-2 (Takasugi *et al*, 2003). PS serves as the catalytic subunit of γ-secretase, in which a pair of aspartate residues located on the N- and C-terminal endoproteolytic fragments of PS (NTF and CTF, respectively) comprise the catalytic site. A series of chemical biology experiments revealed that all GSIs investigated so far directly target PS (Tomita, 2009). However, the molecular target, as well as the mechanism of action, of GSMs remains enigmatic. A couple of recent studies suggested that NSAID-based GSMs directly and specifically target APP, but not the enzyme (i.e., γ-secretase; Kukar *et al*, 2008). In contrast, several lines of evidence suggest that the effects of GSM are not limited to the γ-secretase cleavage of APP: it has been shown that some GSMs modulated the C-terminal length of Nβ, a proteolytic product of Notch corresponding to Aβ (Okochi *et al*, 2006), and the activity of signal peptide peptidase (SPP), a PS-type intramembrane cleaving protease with an inverse orientation of the catalytic structure, also was affected by NSAIDs (Sato T *et al*, 2006). Moreover, reports casting doubt to the substrate targeting of NSAIDs have recently been published (Beel *et al*, 2009; Page *et al*, 2010). However, there has not been direct and conclusive evidence regarding the target of the GSMs.

Here, we examined the target and mode of action of GSM-1, one of the representative Aβ42-lowering GSMs harbouring a phenylpiperidine structure (Page *et al*, 2008). Using two novel photoprobes derivatized from GSM-1, we have unequivocally located the binding site of the phenylpiperidine-type GSM on a subdomain within the transmembrane domain (TMD) 1 of PS1, which has been shown to participate in the catalytic pore structure of γ-secretase (Takagi *et al*, 2010).

*Corresponding authors. T Tomita or T Iwatsubo, Department of Neuropathology and Neuroscience, Graduate School of Pharmaceutical Sciences, The University of Tokyo, 7-3-1 Hongo, Bunkyo-ku, Tokyo 113-0033, Japan. Tel.: +81 3 5841 4895; Fax: +81 3 5841 4708; E-mail: taisuke@mol.f.u-tokyo.ac.jp or iwatsubo@m.u-tokyo.ac.jp

Received: 29 May 2011; accepted: 21 September 2011; published online: 14 October 2011

Our results suggest that GSM-1 decreases the production of Aβ42 possibly by enhancing its conversion to Aβ38, by an allosteric mechanism by binding to the TMD1 of PS1.

Results

GSM-1 affects the Aβ38- and Aβ42-generating activities of γ-secretase

GSM-1 is a phenylpiperidine-type compound that shows a potent Aβ42-lowering effect ($IC_{50} = 0.348\,\mu M$ in a cell-based assay) accompanied by an increased production of Aβ38 (Figure 1A), as documented (Page *et al*, 2008). Recent biochemical studies suggest that γ-secretase executes a stepwise removal of tripeptides from the C termini of longer Aβ species that are cognate precursors for secreted form of Aβ: Aβ40 and Aβ42 are successively derived from Aβ43/46/49 and Aβ45/48, respectively (Qi-Takahara *et al*, 2005; Takami *et al*, 2009). An additional cleavage of Aβ42 generates Aβ38. To further characterize the effect of GSM-1 on the stepwise γ-secretase cleavage leading to Aβ secretion, we examined the production of the different Aβ species (i.e., Aβ38, Aβ40, Aβ42, Aβ43, Aβ45 and Aβ46) in an *in-vitro* assay. The levels of total Aβ and its C-terminal counterpart product, APP intracellular domain (AICD), were not affected by GSM-1 treatment (Supplementary Figure S1A–C). However, GSM-1 selectively reduced the Aβ42 generation accompanied by an increase in Aβ38, similarly to the results in the cell-based assay (Figure 1B and C). Notably, generation of Aβ45, a hypothetical precursor of Aβ42 and Aβ38, was not affected. These data suggest that GSM-1 exclusively affected the γ-cleavage that cuts the midst of the TMD of substrates, but not the ε- or ζ-cleavages (corresponding to the production of AICD/Aβ48/49 and Aβ45/46, respectively) that occur at positions closer to the cytoplasm. To ascertain that GSM-1 directly affects the γ-cleavage, we examined the effect of GSM-1 in an *in-vitro* γ-secretase assay using reconstituted γ-secretase complex recovered from Sf9 cells infected with recombinant baculovirus (Hayashi *et al*, 2004; Ogura *et al*, 2006). Again, GSM-1 caused a decrease in the *de novo* generation of Aβ42 and an increase in that of Aβ38, confirming the direct action of GSM-1 on the γ-secretase-mediated cleavage (Figure 1D).

GSM-1 directly binds to the N-terminal fragment of PS1

To identify the molecular target of GSM-1, we employed photoaffinity labelling (PAL; Morohashi *et al*, 2006; Fuwa *et al*, 2007) using photoactivatable probes harbouring photoactivatable and biotin moieties. The molecular target of the probe is covalently crosslinked upon UV irradiation and purified by the avidin-biotin catch principle (Hofmann and Kiso, 1976). We synthesized a GSM-1-based photoactivatable probe, GSM-1-BpB (see Supplementary Scheme 1), in which

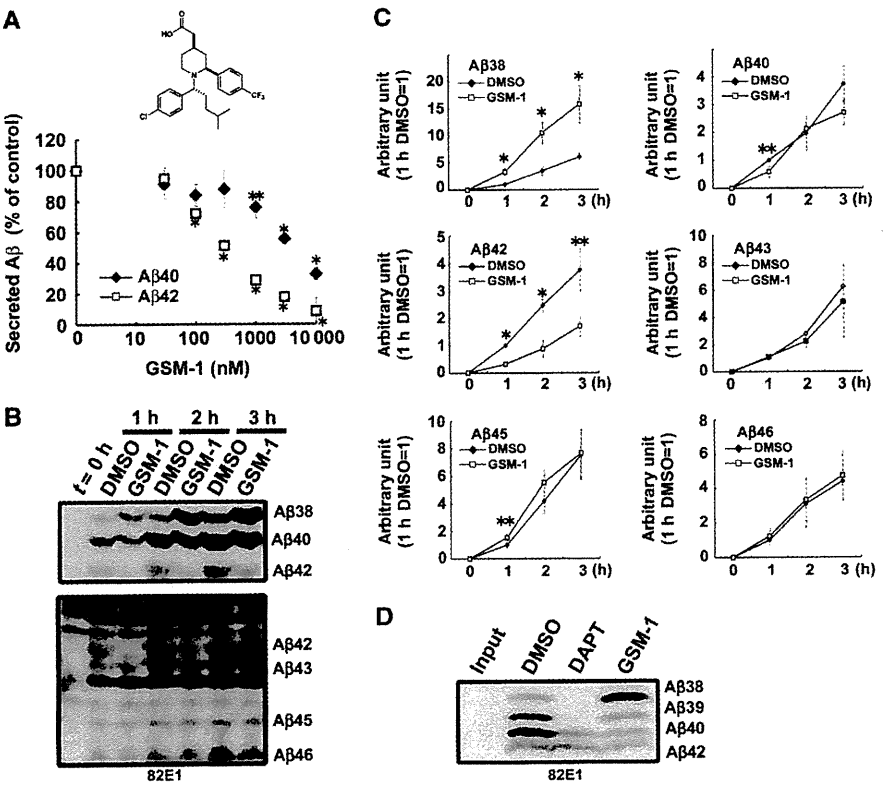

Figure 1 GSM-1 directly and selectively affects the Aβ38/42-generating γ-secretase activity. (**A**) Chemical structure of GSM-1 and its pharmacological effect on a cell-based assay. Aβ levels in conditioned media from HEK293 cells were analysed by ELISAs ($n = 3$, mean ± s.d., $^*P<0.01$, $^{**}P<0.05$ at Student's *t*-test). (**B**) Effect of GSM-1 (25 μM) on stepwise cleavage by γ-secretase in an *in-vitro* assay. *De novo* generated Aβ species were separated by two types of gels (Qi-Takahara *et al*, 2005). (**C**) Quantitation of *de novo* generated Aβ in an *in-vitro* assay ($n = 3$, mean ± s.d., $^*P<0.01$; $^{**}P<0.05$ at Student's *t*-test). (**D**) *De novo* Aβ generation using purified γ-secretase in the presence of DAPT (20 μM) or GSM-1 (20 μM).

benzophenone and biotin moieties were conjugated to GSM-1. GSM-1-BpB retained the Aβ42-lowering (IC_{50} = 3.82 μM in a cell-based assay) and Aβ38-raising activities (Figure 2A and B). Neither GSM-1 nor GSM-1-BpB affected the production of NICD, suggesting that GSM-1-BpB harbours a similar modulator effect to GSM-1 (Figure 2C). Next, we performed the PAL experiments by GSM-1-BpB in mouse brain microsomes, and detected the specific biotinylation of endogenous PS1 NTF, which was decreased by co-incubation with the parent compound GSM-1 (Figure 3A and B). We did not observe labelling of other γ-secretase components, nor of the APP C-terminal stub, by GSM-1-BpB. Specific labelling of PS1 by GSM-1-BpB was also observed in immortalized fibroblasts derived from *Psen1*$^{-/-}$/*Psen2*$^{-/-}$ mice (DKO cells) (Herreman *et al*, 2000) stably expressing His-tagged PS1, supporting the direct targeting of GSM-1 to PS1 NTF (Figure 3C). Moreover, recombinant SPP (Sato T *et al*, 2006; Fuwa *et al*, 2007), a PS family protease, also was directly targeted by GSM-1 and underwent specific modulation of its activity (Supplementary Figure S2A and B). $(Z\text{-}LL)_2$-ketone, well-known SPP-specific inhibitor, unaffected SPP labelling by GSM-1-BpB. Collectively, these data supported the notion that GSM-1 is directly bound to PS-type intramembrane cleaving proteases, and that PS1 NTF is a *bona fide* target of GSM-1.

Phenylpiperidine-type GSMs affect the structure of PS1 NTF in an allosteric manner

Next, we performed cross-competition experiments in PAL using a set of conventional GSIs to examine the effect of GSM-1 binding on the enzymatically functional sites within PS1. We used L-685,458, pep.11 and compound E, which are predicted to target γ-secretase catalytic site, the initial substrate binding site and the transit path between these sites, respectively, as competitors (Li *et al*, 2000; Das *et al*, 2003; Fuwa *et al*, 2007). To ensure a fair competition with the GSM-1-BpB binding, we employed pretreatment with unlabelled competitor compounds at 10-fold concentrations of the IC_{50} values against Aβ42 generation (IC_{50} values: GSM-1, 24.09 μM (Supplementary Figure S3A and B); L-685,458, 0.59 μM; pep.11, 0.48 μM; compound E, 0.97 nM as determined in our cell-free γ-secretase assays). Pretreatment with neither of these three GSIs affected the labelling of PS1 NTF by GSM-1-BpB (Figure 4A). Furthermore, 10 μM of each GSI also unaffected GSM-1-BpB binding (Supplementary Figure

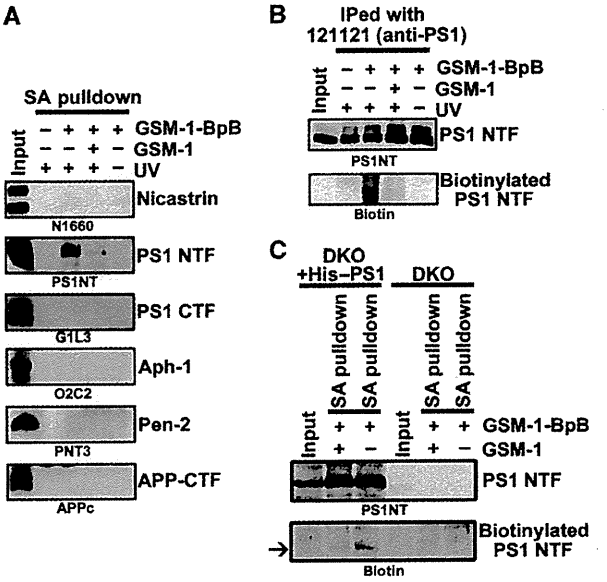

Figure 3 GSM-1-BpB directly binds to PS1 NTF. (**A**) PAL experiments using mouse brain membranes. PS1 NTF was specifically labelled with GSM-1-BpB (1 μM). The labelling was competed by preincubation with GSM-1 (100 μM). (**B**) Direct biotinylation of PS1 NTF. After PAL, PS1 NTF was precipitated using anti-PS1 NTF antibody and analysed by an anti-biotin antibody. (**C**) Biotinylation of His-tagged PS1 expressed in DKO cells by GSM-1-BpB. After PAL, His-tagged PS1 (*arrow*) was purified with Ni^{2+}-affinity column and analysed by immunoblotting.

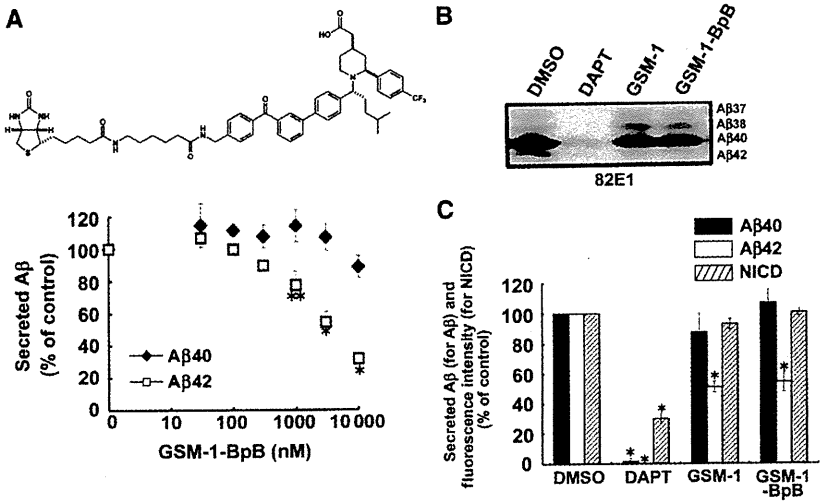

Figure 2 GSM-1-BpB harbours Aβ42-lowering modulator activity. (**A**) Chemical structure of GSM-1-BpB and its pharmacological effect on a cell-based assay (n = 3, mean ± s.d., $^*P<0.01$, $^{**}P<0.05$ at Student's t-test). (**B**) Immunoblotting analyses of conditioned media from HEK293 cells in the presence of DAPT (10 μM), GSM-1 (2 μM) or GSM-1-BpB (2 μM). (**C**) Effects on Notch cleavage of DAPT (10 μM), GSM-1 (0.3 μM) or GSM-1-BpB (3 μM) (n = 3, mean ± s.d., $^*P<0.01$, $^{**}P<0.05$ at Student's t-test).

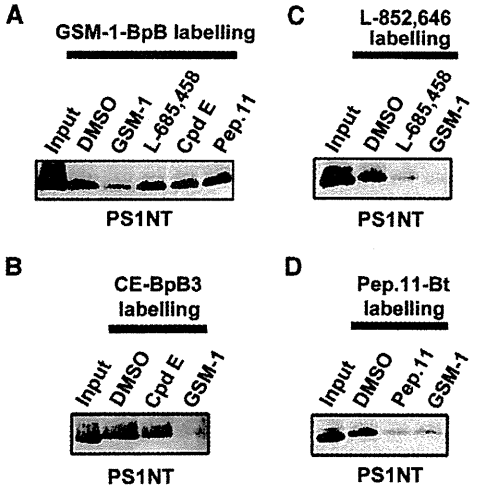

Figure 4 Competition of the photoaffinity labelling of PS1 NTF by GSM-1-BpB. (**A**) Labelling competition experiment with conventional GSIs for the labelling of PS1 NTF by GSM-1-BpB. GSIs were tested at the 10-fold concentration of IC_{50} (final concentrations: compound E (Cpd E) (9.7 nM), L-685,458 (5.9 μM) and pep.11 (4.8 μM)). (**B–D**) Labelling competition experiments with GSM-1 (240.9 μM) for the labelling of PS1 NTF by CE-BpB (**B**), L-852,646 (**C**) and pep.11-Bt (**D**).

S4A), indicating that the binding site of GSM-1 is distinct from those of the conventional GSIs. In contrast, pretreatment with GSM-1 significantly inhibited the labelling of PS1-NTF by CE-BpB3, L-852,646 and pep.11-Bt, which are photoprobes derived from compound E, L-685,458 and pep.11, respectively (Figure 4B–D). Importantly, GSM-1 showed no competition on the labelling by DAP-BpB, which has been known to target PS1 CTF (Morohashi *et al*, 2006), ensuring the specificity of the competition by GSM-1 (Supplementary Figure S4B). We further examined the effects of γ-secretase substrates on GSM-1-BpB labelling, since other classes of GSMs (i.e., ibuprofen and fenofibrate) have been suggested to dock with PS in the presence of substrates (Uemura *et al*, 2010). Notably, labelling of GSM-1-BpB was altered neither by pretreatment with a substrate-mimetic inhibitor pep.11 (Figure 4A), nor by overexpression of C99, an APP-based substrate (Supplementary Figure S5), indicating that GSM-1 specifically bound to PS1 NTF independent of substrate binding. These data support the notion that binding of GSM-1 to PS1 NTF affects the structures of enzymatically functional sites within PS1.

Through the structure–activity relationship analysis of GSM-1, we found that the carboxylic acid moiety is critical for the Aβ42-lowering effect. Among the derivatives, NS-1017 (See Supplementary Scheme 2), which harbours an *N*-benzylamide moiety showed a significant Aβ42-raising effect associated with decreased Aβ38 production (Figure 5A and B). Intriguingly, preincubation with NS-1017 diminished the labelling of PS1 NTF by GSM-1-BpB (Figure 5C), suggesting that the phenylpiperidine structure is the pharmacophore that targets the modulator binding site within PS1 NTF, and that the substituent at the 4-position of the piperidine (i.e., carboxylic acid or amide) determines the pharmacological effects on Aβ42 production. We also synthesized a phenylpiperidine-type Aβ42-raising photoprobe, GSM-1-amide-BpB (See Supplementary Scheme 3), in which the biotin-benzo-

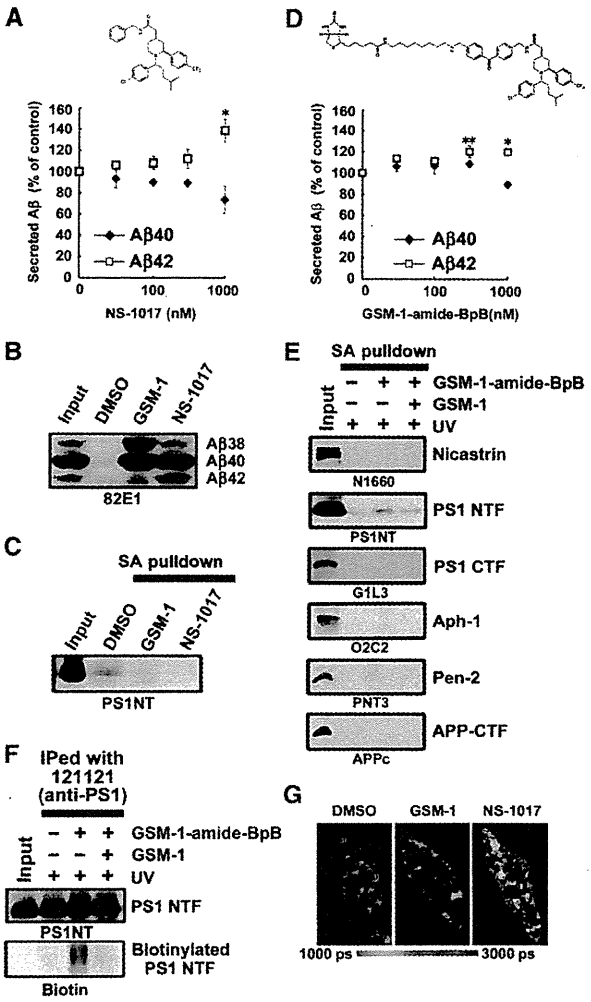

Figure 5 Aβ42-raising phenylpiperidine-type modulator directly targets PS1 NTF. (**A**) Chemical structure of NS-1017 and its pharmacological effect on a cell-based assay ($n=3$, mean ± s.d., $^*P<0.01$ at Student's *t*-test). (**B**) Immunoblot analysis of secreted Aβ in conditioned media in the presence of DAPT (10 μM), GSM-1 (2 μM) or NS-1017 (2 μM). (**C**) Labelling competition experiment with GSM-1 (100 μM) or NS-1017 (200 μM) for the GSM-1-BpB labelling of PS1 NTF (1 μM) using mouse brain microsomes. (**D**) Chemical structure of GSM-1-amide-BpB and its pharmacological effect on a cell-based assay ($n=3$, mean ± s.d., $^*P<0.01$, $^{**}P<0.05$ at Student's *t*-test). (**E**) PAL experiment using GSM-1-amide-BpB (1 μM) in mouse brain microsomes. (**F**) Immunoprecipitated PS1 NTF was analysed by an anti-biotin antibody after PAL in mouse brain microsomes. (**G**) Effects of GSM-1 and NS-1017 on the structure of PS1 revealed by FLIM assay. Pseudo-coloured FLIM images showed subcellular distribution of the GFP lifetimes, with red pixels representing shorter lifetime (closer GFP-PS1 NT and RFP-PS1-loop proximity). A colorimetric scale bar shows colour-coded fluorescence lifetime in picoseconds.

phenone moiety was directly connected to the amide moiety (Figure 5D). GSM-1-amide-BpB also specifically biotinylated PS1 NTF in mouse brain membranes, supporting the notion that the phenylpiperidine structure is required for the targeting to the modulator binding site (Figure 5D and E).

Using fluorescence lifetime imaging microscopy (FLIM), we have previously reported that the mature PS1 within the active γ-secretase complex exists in equilibrium between two conformational states: 'open' and 'closed' NTF/CTF confor-

Table I Differences in the proximity between N- and C-termini of PS1 shown by FLIM assay

Construct	Compound	Av lifetime	s.d.	*n*	*t*-test versus PS1 DMSO
GFP-PS1-RFP	DMSO	1872.4	144.3	61	—
GFP-PS1-RFP	GSM-1	1921.0	114.0	54	0.0463*
GFP-PS1-RFP	NS-1017	1812.4	154.1	71	0.0388*

*$P<0.05$ versus GFP-PS1-RFP DMSO (Student's *t*-test).

mations that correspond to the low and high ratio of Aβ42/Aβ40 production, respectively (Lleo *et al*, 2004; Uemura *et al*, 2009). By FLIM, we found that GSM-1 treatment leads to a significant increase in the GFP lifetime in cells expressing PS1 fused with GFP and RFP at the N-terminus and within large hydrophilic loop of PS1 CTF, respectively. This indicates that GSM-1 treatment caused an 'open-form' PS1 conformation similar to that caused by Aβ42-loweirng NSAID-type GSMs. Interestingly, NS-1017 had an opposite effect on PS1, and similarly to fenofibrate led PS1 to exhibit the 'close-form' conformation (Figure 5G; Table I; Lleo *et al*, 2004; Uemura *et al*, 2009). These data indicate that the phenylpiperidine-type GSMs modulated γ-cleavage through conformational changes of PS1 by interacting with a common binding site.

The TMD1 of PS1 is required for the binding of GSM-1

FLIM results suggested a conformational change of PS1 that results in altered proximity between the N-terminus and loop domain of PS1. However, we found that PS1 mutant lacking the N-terminal amino-acid residues from Thr2 to Ala79 (PS1Δ79) retained the sensitivity to GSM-1 in DKO cells (Supplementary Figure S6A–C). In addition, phenylpiperidine-type GSMs were effective on γ-secretase complex containing PS2 with a low sequence similarity to PS1 at the N-terminus (Supplementary Figure S6D and E). These data indicated that the N-terminal cytoplasmic domain of PS1 is dispensable to the pharmacological effect of GSM-1. To further narrow down the binding site of GSM-1 within the PS1 NTF, we have taken a limited digestion approach: we inserted a thrombin substrate sequence (i.e., LVPRGS) into the hydrophilic regions within PS1 NTF (i.e., PS1-Th60N at the N-terminus, PS1-Th1 and PS1-Th3 at the loops 1 and 3, respectively; Figure 6A), and confirmed that overexpression of these mutants in DKO cells restored the γ-secretase activity that was modulated by GSM-1 (Figure 6B; Supplementary Figure S7). Proteolytic cleavage of PS1-Th60N, PS1-Th1 and PS1-Th3 mutants by thrombin resulted in generation of 8, 12 and 23 kDa N-terminal fragments of PS1 NTF, respectively, which are detectable by the anti-PS1 N-terminus antibody (Figure 6C). To pinpoint the modulator binding domain within PS1 NTF, we subjected these mutants to thrombin treatment after PAL with GSM-1-BpB (Figure 6D). N-terminal fragments derived from PS1-Th1 or PS1-Th3 were pulled down by streptavidin beads, but that from PS1-Th60N was not (Figure 6D). Furthermore, preincubation with GSM-1 reduced the labelling of the cleaved fragment of PS1-Th1 (Figure 6E). These data suggest that the GSM-1 binding site resides within the region between Lys80 and Asp110.

Using CHO cells in which holoprotein form of endogenous PS1 was detectable, we found that GSM-1-BpB and GSM-1-amide-BpB specifically labelled the PS1 holoprotein (Supplementary Figure S8A and B). PS1 mutant carrying the protease-inactive D385A mutation also was labelled. These data suggest that GSM-1 binds to PS1 irrespective of the formation of the stable γ-secretase complex or the proteolytic activity. Taking advantage of these features, we examined the labelling of TMD-swap mutants of PS1, in which each TMD was replaced with that of an unrelated transmembrane protein, CLAC-P, with a proper orientation. These TMD-swap mutants failed to exhibit the enzyme activities, although forming the γ-secretase complex (Watanabe *et al*, 2005, 2010). TM1mt PS1, in which amino-acid residues Val82 to Ile100 of PS1 were replaced, failed to be labelled by GSM-1-BpB, whereas TM5mt and TM9mt PS1 were biotinylated (Figure 6F). To further verify the specificity of binding of GSM-1-BpB to the TMD1 of PS1, we subjected purified recombinant glutathione S-transferase (GST), GST fused protein of $PS1_{2-65}$ or $PS1_{1-110}$ to PAL with GSM-1-BpB (Figure 6G; Supplementary Figure S9). Notably, photolysis of GSM-1-BpB resulted in the specific binding exclusively to GST-$PS1_{1-110}$ encompassing the TMD1, but not to GST-$PS1_{2-65}$ corresponding to the N-terminal cytoplasmic portion of PS1, indicating the requirement of TMD1 for the binding of GSM-1-BpB (Figure 6H). Collectively, these data suggest that TMD1 is the binding site of phenylpiperidine-type GSMs.

GSM-1 targets the hydrophobic portion of the TMD1 of PS1 and allosterically affects the conformation of PS1

To further characterize the structural changes of TMD1 of PS1 caused by binding of GSM-1, we utilized substituted cysteine accessibility method (SCAM), a biochemical analysis of the structures of membrane proteins in a membrane-embedded, functional state, by assessing the hydrophilicity of each amino-acid residue by the biotinylation efficiency of mutated cysteine at the same position. We have previously shown that TMD1 of PS1, comprising residues Gly78 to Ile100, faces a hydrophilic environment within the membrane by SCAM (Takagi *et al*, 2010). TMD1 consists of two functional regions: the N-terminal portion close to the cytoplasm is facing the catalytic site of the γ-secretase, whereas the C-terminal portion is buried within the lipid bilayer and possibly involved in the structural integrity of PS1 via hydrophobic interactions with other TMDs. The results of PAL and FLIM experiments suggested that a conformational change of TMD1 was linked to the modulator activity of GSMs. Intriguingly, mutant PS1 replaced with the amino-acid sequences of CLAC-P at this hydrophilic segment (i.e., Val82 to Pro88) retained the γ-secretase activity as well as the sensitivity to the modulatory effect of GSM-1, suggesting that the C-terminal side, rather than the N-terminal side, of TMD1 harbours the modulator binding site (Supplementary Figure S10A–C). These observations further prompted us to analyse the effect of GSM-1 on the water accessibility of the six residues within TMD1 (i.e., Lys80, His81, Val82, Ile83, Met84 and Leu85), which directly face the hydrophilic environment by SCAM. We have previously shown that competition of SCAM labelling is useful for the identification of the binding site, or the allosteric effect, of small compounds (Sato C *et al*, 2006, 2008; Takagi *et al*, 2010). Treatment with either GSM-1 or NS-1017 slightly, but constantly reduced the labelling of single-cysteine PS1 mutant at Met84 (M84C), whose labelling has never been affected by competition with conventional GSIs (Takagi *et al*, 2010). In addition, NS-1017 reduced the labelling of K80C (Figure 7A). In contrast, the labelling of other hydrophilic residues in TMD1, as well as of residues forming the

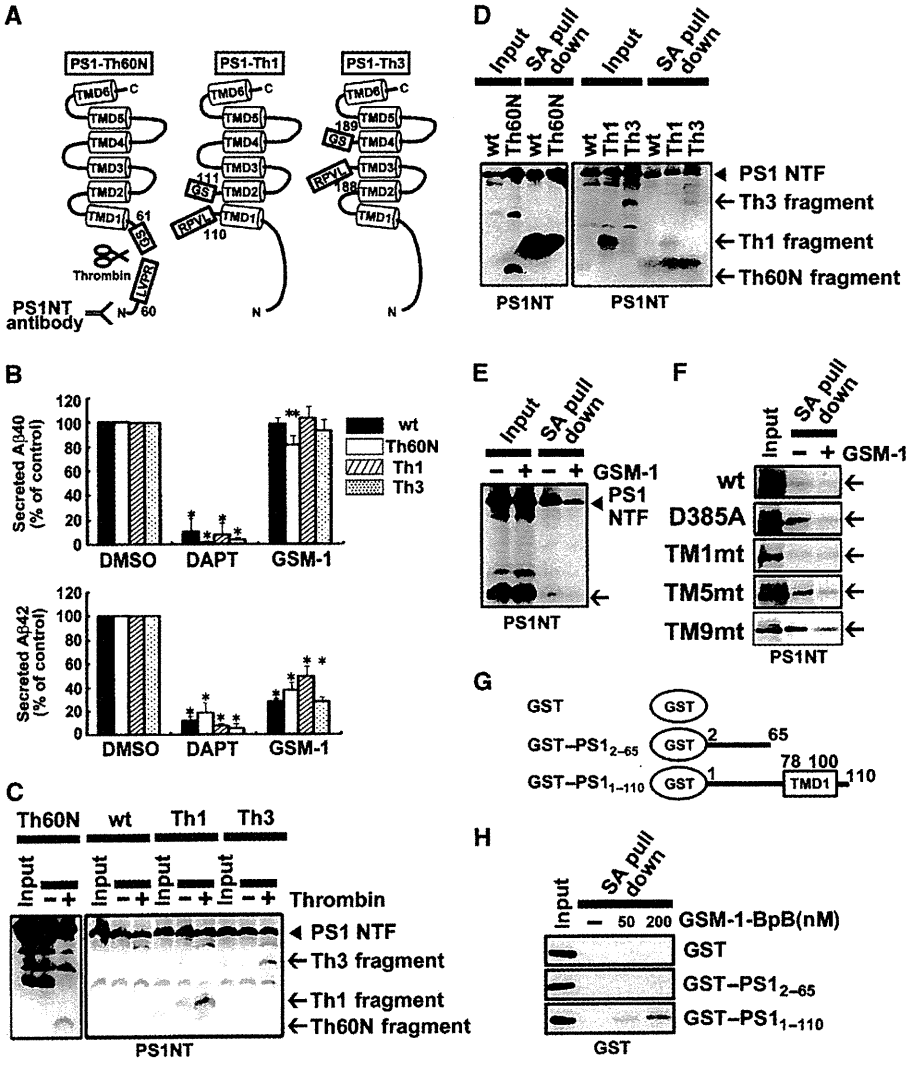

Figure 6 Identification of TMD1 of PS1 as the binding site of GSM-1-BpB. (**A**) Schematic representation of the NTF of mutant PS1 inserted with a thrombin-cleavage sequence (squares) at different sites (PS1-Th60N, PS1-Th1 and PS1-Th3). (**B**) Effect of DAPT (10 μM) or GSM-1 (1 μM) on secreted Aβ from DKO cells stably expressing APPNL and PS1 mutants ($n=3$, mean ± s.d., $^*P<0.01$, $^{**}P<0.05$ at Student's *t*-test). (**C**) Thrombin digestion experiments of PS1-Th60N, PS1-Th1 and PS1-Th3. PS1 NTF and the cleaved fragments were indicated by an *arrow* and *arrowheads*. (**D**) Thrombin digestion experiments after PAL by GSM-1-BpB (1 μM). Note that cleaved Th1 or Th3 fragment, but not Th60N fragment, was precipitated and detected by anti-PS1 NTF antibody. (**E**) Preincubation by GSM-1 (200 μM) decreased the labelling of both PS1 NTF (*arrowhead*) and Th1 fragment (*arrow*). (**F**) PAL experiment of TM-swap mutant PS1 by GSM-1-BpB (1 μM). GSM-1-BpB labelled holoprotein forms of PS1 (*arrows*). Note that TM1mt PS1 was never labelled by GSM-1-BpB. (**G**) Schematic representation of recombinant proteins used in this study. (**H**) PAL experiment for recombinant proteins by GSM-1-BpB. Recombinant GST-PS1$_{1-110}$, but not GST or GST-PS1$_{2-65}$ (0.5 μg each), was labelled by GSM-1-BpB in a dose-dependent manner.

catalytic site in TMD6 (i.e., A246C and L250C; Sato C *et al*, 2006) was not altered by phenylpiperidine-type GSMs (Figure 7A and B). These data indicate that the water accessibility of the cytosolic side of TMD1 is specifically altered by the binding of phenylpiperidine-type GSMs. Taken altogether, we conclude that the phenylpiperidine-type GSMs directly and specifically target the TMD1 of PS1, leading to an alteration in the conformation of the catalytic pore structure of the γ-secretase, and thereby modulating the Aβ42 production (Figure 7C).

Discussion

By a combination of chemical biology and molecular biology approaches, we have identified TMD1 of PS1 as the binding site of GSM-1, a representative and potent Aβ42-lowering GSM (Page *et al*, 2008). GSM-1 bound to PS1 either in an inactive, holoprotein form or within an enzymatically active complex, and induced conformational changes in the catalytic as well as the initial substrate binding sites in PS1. Thus, the mode of binding of GSM-1 to PS1 is different from that of the conventional GSIs, which selectively target the enzymatically active form of PS1 (Li *et al*, 2000; Morohashi *et al*, 2006; Fuwa *et al*, 2007; Watanabe *et al*, 2010). SCAM assay revealed that phenylpiperidine-type GSMs affected the water accessibility of Met84 located at the N-terminal region of TMD1 (Figure 7A). Notably, we have previously shown that Val82 and Leu85 in TMD1 of PS1 directly participate in the formation of the catalytic site of γ-secretase, while Met84

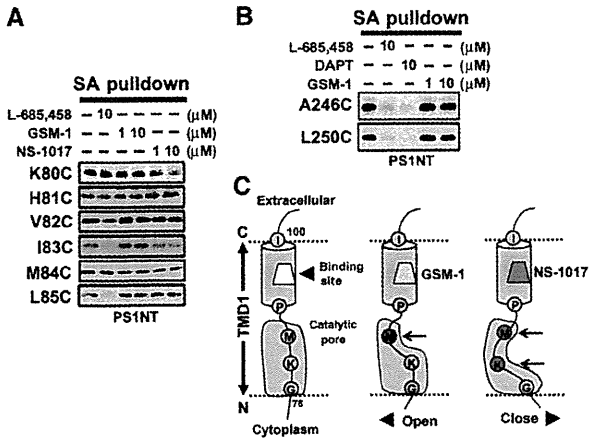

Figure 7 Conformational changes in the cytoplasmic side of TMD1 of PS1 induced by phenylpiperidine-type γ-secretase modulators. (**A**, **B**) SCAM analysis of microsomes from DKO cells expressing single-Cys mt PS1 containing one Cys at the cytosolic side of TMD1 (**A**) or TMD6 (**B**) in the presence or absence of indicated compounds. All bands correspond to the biotinylated PS1 NTF. Note that the labelling of K80C or M84C was affected by preincubation with GSM-1 or NS-1017. (**C**) A hypothetical model of mode of action of phenylpiperidine-type GSMs. Membrane borders are indicated by dotted lines. N-terminal domain of TMD1 facing the catalytic pore is indicated by a blue region. C-terminal domain of TMD1 is shown by a pink cylinder. Yellow and red trapezoids indicate GSM-1 and NS-1017, respectively. The hypothetical open and close structure of the N-terminal domain of TMD1 of PS1 induced by GSMs is indicated.

does not, consistent with the notion that the phenylpiperidine-type GSMs affect the catalytic site in an allosteric manner. In addition to Met84, Aβ42-rasing NS-1017 decreased the water accessibility of Lys80, suggesting that a specific structural change around this region is linked to alteration in the net production of Aβ42 (Figure 7A and C). Interestingly, several FAD-linked mutations have been identified in the N-terminal region of TMD1 of PS1, suggesting that conformational changes in this region may be an important determinant for the Aβ42 generating activity. In contrast, analyses of the swap mutants revealed that the cytosolic side of TMD1 was dispensable for the binding of GSM-1. These data suggest that the phenylpiperidine-type GSMs directly target the hydrophobic C-terminal half of TMD1 (Figure 7C). Intriguingly, this hydrophobic half participates in the maintenance of the TMD-to-TMD interaction in PS1, which is involved in the assembly of the γ-secretase complex as well as the mechanism of substrate recognition (Takagi *et al*, 2010; Watanabe *et al*, 2010). Our data provide compelling evidence supporting the notion that phenylpiperidine-type GSMs modulate the γ-secretase activity by directly targeting the hydrophobic extracellular/luminal side of the PS1 TMD1, leading to a conformational change of the hydrophilic cytosolic side (Figure 7A and C).

Biochemical analyses indicate the presence of two product lines by γ-secretase to generate Aβ40/43 and Aβ38/42 from Aβ49 and Aβ48, respectively (Qi-Takahara *et al*, 2005; Takami *et al*, 2009). Here, we showed that only the Aβ38/42-generating activity was modulated by GSM-1 without affecting the levels of AICD as well as of other Aβ species including Aβ45, the latter being the possible cognate precursor for Aβ42. This is consistent with the previous findings that an NSAID-type GSM, sulindac sulphide, exclusively increased the release of tetrapeptide VVIA, which is derived from Aβ42 upon generation of Aβ38 (Takami *et al*, 2009). These results lead us to speculate that the Aβ42-lowering GSMs selectively alter the proteolytic activity upon the stepwise cleavage to generate Aβ38. The decrease in the binding of L-852,646 (a transition state analogue photoprobe) by GSM-1 reflects a structural change in the catalytic site. In contrast, Aβ40 generation was never affected by GSM-1. Notably, alignments of scissile bonds in the two product lines (i.e., Aβ49-46-43-40 and Aβ48-45-42-38) are located on distinct interfaces of the α-helical model of the substrate (Qi-Takahara *et al*, 2005; Takami *et al*, 2009). However, the result that GSM-1 decreased the labelling of PS1 NTF by pep.11-Bt may indicate an allosteric effect on the structure of the initial substrate binding site that determines Aβ42 generation. Thus, the selective modulation of Aβ38/42 generation suggests that GSM-1 affects both the catalytic pocket and the recognition mechanism of the helical interface during the processive cleavage of Aβ48/45/42.

A subset of NSAID-type GSMs have been reported to directly target the TMD of APP, especially the GXXXG motif (Kukar *et al*, 2008; Richter *et al*, 2010). However, this notion contradicts with the previous findings that several GSMs modulate the γ-secretase-mediated cleavage of substrates other than APP (i.e., Notch); these GSMs affect the cleavage of APP mutated at the GXXXG motif too (Okochi *et al*, 2006; Page *et al*, 2010). Moreover, the activity of SPP, a protease homologous to γ-secretase, also was affected by GSMs (Sato T *et al*, 2006). In this study, we demonstrated the direct biotinylation of PS1 NTF as well as of SPP by GSM-1-BpB, suggesting that the phenylpiperidine-type GSM bound to these enzymes. However, it remains possible that GSMs target the interface between the enzyme and the substrate upon modulation of the Aβ42 production. In this case, GSM might form a tripartite complex with the PS1 TMD1 and the substrate (Uemura *et al*, 2010). In fact, both the hydrophobic region of TMD1 of PS1 and the GXXXG motif in APP TMD are predicted to be located at similar topological position within the lipid bilayer: dual roles of TMD1 in the γ-secretase-mediated cleavage (i.e., substrate recognition as well as catalytic reaction) fit with this hypothesis (Takagi *et al*, 2010). However, we are not able to exclude the possibility that different domains of PS1 or other γ-secretase subunits are also involved in the modulation of Aβ42 generation, since PAL detects the closest target molecule located in proximity to the photoactivatable moiety. Intriguingly, we previously reported that the N-terminus of Pen-2, which is directly bound to TMD4 of PS1 (Watanabe *et al*, 2005), is involved in the selective modulation of Aβ42 production as well as the conformation of PS1 (Isoo *et al*, 2007; Uemura *et al*, 2009). And recently, a GSM with a phenylimidazole pharmacophore was reported to primarily target Pen-2 (Kounnas *et al*, 2010). In this regard, it is tempting to speculate that TMD1 and TMD4 of PS1, together with Pen-2, form the modulator binding site in the γ-secretase complex. It is also possible that different types of GSMs show distinct preference of interaction with γ-secretase components or substrates. Further detailed structural analysis (i.e., X-ray crystallography or NMR) of PS1, in a state coupled with a GSM and a substrate, would be required for the understanding of a variety in the molecular action of different GSMs.

In sum, we revealed the specific molecular action of the phenylpiperidine-type GSMs on PS1 TMD1 using a comprehensive strategy based on chemical biology. Such an approach would be useful for the rational design of small compounds in the development of effective therapeutics for AD.

Materials and methods

Compounds, peptides and antibodies

GSM-1, GSM-1-BpB, NS-1017 and GSM-1-amide-BpB were synthesized as described in Supplementary data. DAPT was synthesized as previously described (Morohashi *et al*, 2006). $(Z\text{-}LL)_2$-ketone, compound E, L-685,458, pep.11 and pep.11-Bt were purchased from Calbiochem, Bachem, Peptide Institute, Inc. and Ito Lifescience, respectively. CE-BpB3 (Fuwa *et al*, 2007) and L-852,646 (Li *et al*, 2000) were kindly provided from Drs H Fuwa (Tohoku University) and Y Li (Sloan-Kettering Cancer Center). The rabbit polyclonal antibodies anti-PS1 CTF (G1L3) and anti-Pen2 (PNT3) were raised as described (Tomita *et al*, 1999; Isoo *et al*, 2007). Anti-GST rabbit polyclonal antibody was purified using Glutathione sepharose 4B (GE Healthcare). Anti-PS1 NTF (PS1NT) and anti-SPP (SPPc) were kindly gifted from Drs G Thinakaran (University of Chicago) and T Golde (Universtiy of Florida). Anti-PS1-NTF 121121 (R&D Systems), anti-nicastrin N1660 (Sigma), anti-APP-CTF (Immuno-Biological Laboratories), anti-Aph-1aL O2C2 (Covance), anti-myc 9B11 (Cell Signaling Technology), anti-human Aβ 82E1 (Immuno-Biological Laboratories) and anti-biotin (Bethyl) were purchased from indicated vendors. The monoclonal antibody anti-α-tubulin AA4.3 developed by Dr C Walsh was obtained from the Developmental Studies Hybridoma Bank developed under the auspices of the NICHD, National Institutes of Health, and maintained by The University of Iowa, Department of Biology, Iowa City, IA.

Plasmid construction and cell culture manipulation

cDNAs encoding mutant PS1 were generated by long PCR-based QuikChange™ strategy (Stratagene). cDNAs encoding PS1, APP carrying Swedish mutation (APPNL) and NotchΔE (Kopan *et al*, 1996) were inserted into pMXs-puro (Kitamura *et al*, 2003). For construction of the thrombin-cleavable PS1 mutant, thrombin-cleavage sequence (CTGGTTCCGCGTGGATCC) was inserted into PS1 cDNA in pMXs-puro. To produce recombinant proteins, cDNAs encoding $PS1_{2\text{-}65}$ and $PS1_{1\text{-}110}$ were cloned into pGEX-6P-1 vector (GE Healthcare). Maintenance of cultured cells and infection of recombinant viruses were done as previously described (Hayashi *et al*, 2004; Watanabe *et al*, 2005, 2010; Morohashi *et al*, 2006; Ogura *et al*, 2006; Sato C *et al*, 2006; Fuwa *et al*, 2007; Takagi *et al*, 2010).

Cell-based, cell-free and in-vitro γ-secretase assay

Immunoblot analysis was performed as previously described (Tomita *et al*, 1997, 1999). To monitor the cleavage of Notch, luciferase assay using HEK293 cells stably expressing APPNL/NotchΔE/EGFP/UAS-firefly luciferase was performed as previously described (Isoo *et al*, 2007; Imamura *et al*, 2009). For secreted Aβ levels, conditioned media from DKO cells co-expressing APPNL and PS1 mutant were analysed by two-site enzyme-linked immunosorbent assay (ELISA; Tomita *et al*, 1997) or immunoblotting using Urea/SDS-PAGE gel system as described (Qi-Takahara *et al*, 2005; Kakuda *et al*, 2006; Osawa *et al*, 2008). For cell-free γ-secretase assay, membranes of CHO cells stably expressing C99 were collected and analysed as described previously (Kakuda *et al*, 2006; Osawa *et al*, 2008). In all, 2.5 mg/ml microsomes in homogenized buffer (20 mM HEPES (pH 7.0), 140 mM KCl, 250 mM sucrose, 1 mM EGTA) containing 0.5 mM DIFP, 0.5 mM PMSF, 1 μg/ml TLCK, 1 μg/ml antipain, 1 μg/ml leupeptin, 10 μg/ml phosphoramidon, 1 mM EGTA, 5 mM EDTA were preincubated with various compounds on ice for 30 min. Following, microsomes were incubated at 37°C for 6 h. For detection of the γ-secretase activity in solubilized condition, 1% CHAPSO-solubilized membranes were co-incubated with APP-based recombinant substrate under 0.25% CHAPSO condition (Takahashi *et al*, 2003) and then analysed by immunoblot analysis. Recombinant γ-secretase complex as well as SPP was purified from baculovirus-infected Sf9 cells as previously described (Hayashi *et al*, 2004; Kakuda *et al*, 2006; Ogura *et al*, 2006; Fuwa *et al*, 2007). CHO cells expressing C99 and APP-based recombinant substrate were kindly provided from Drs S Funamoto and Y Ihara (Doshisha University). IC_{50} values were calculated by plotting data on Kyplot software (Kyens Lab. Inc.).

PAL, SCAM and FLIM experiments

Membranes from C57J/B6 mouse brain (3–5-month age) and cultured cells were homogenized with homogenize buffer and collected as described (Kakuda *et al*, 2006). PAL experiment utilizing avidin-biotin catch principle (Hofmann and Kiso, 1976) was performed as previously described (Morohashi *et al*, 2006; Fuwa *et al*, 2007; Imamura *et al*, 2009). For thrombin digestion after PAL, recentrifuged pellets were solubilized in thrombin digestion buffer (50 mM Tris–HCl (pH 7.5), 150 mM NaCl, 1 mM EDTA, 1% Triton X-100). After incubation with 5 U/ml thrombin protease (GE Healthcare) at 37°C for 4 h, SDS was added to stop the enzymatic reaction. The biotinylated polypeptides were collected by streptavidin-Sepharose HP (GE Healthcare). For SCAM, all methanethiosulphonate reagents (Toronto Research Chemicals) were dissolved in dimethyl sulphoxide (DMSO) at 200 mM prior to use or stored at 80°C until use. The methods for SCAM and competition experiments using biotinylaminoethyl methanethiosulphonate have been described in detail before (Sato *et al*, 2006, 2008; Takagi *et al*, 2010). The proximity between the N-terminus and TM6-7 loop domain as an indicator of PS1 conformation was monitored by FLIM assay at the cell periphery of live cells expressing GFP-PS1-RFP construct as previously described (Uemura *et al*, 2009, 2010).

Supplementary data

Supplementary data are available at *The EMBO Journal* Online (http://www.embojournal.org).

Acknowledgements

We are grateful to Drs R Kopan (Washington University in St Louis), G Thinakaran (The University of Chicago), T Golde (University of Florida), B De Strooper (VIB Leuven), H Fuwa (Tohoku University) and Y Li (Sloan-Kettering Cancer Center), T Kitamura (The University of Tokyo), S Funamoto and Y Ihara (Doshisha University) for valuable reagents, Takeda pharmaceutical company for Aβ ELISA, and our current and previous laboratory members for helpful discussions and technical assistance. This work was supported in part by grants-in-aid for Young Scientists (S) from the Japan Society for the Promotion of Science (JSPS) (TT), Scientific Research on Priority Areas Research on Pathomechanisms of Brain Disorders from the Ministry of Education, Culture, Sports, Science and Technology, Japan (TT and TI), by the Program for Promotion of Fundamental Studies in Health Sciences of the National Institute of Biomedical Innovation (TT and TI), by Targeted Proteins Research Program of the Japan Science and Technology Corporation (JST) (SY, TF, TT and TI), by Core Research for Evolutional Science and Technology of JST (SY, TF, TT and TI), Japan, and by NIH AG15379 (OB). YO and TH are research fellows of JSPS.

Author contributions: YO and TT designed the research. YO, SO and TT performed biochemical experiments. SY, TH, NS and TF synthesized the compounds. KU and OB performed the imaging experiments. YO, TT and TI wrote the paper.

Conflict of interest

The authors declare that they have no conflict of interest.

References

Beel AJ, Barrett P, Schnier PD, Hitchcock SA, Bagal D, Sanders CR, Jordan JB (2009) Nonspecificity of binding of γ-secretase modulators to the amyloid precursor protein. *Biochemistry* **48:** 11837–11839

Das C, Berezovska O, Diehl TS, Genet C, Buldyrev I, Tsai JY, Hyman BT, Wolfe MS (2003) Designed helical peptides inhibit an intramembrane protease. *J Am Chem Soc* **125:** 11794–11795

De Strooper B, Vassar R, Golde T (2010) The secretases: enzymes with therapeutic potential in Alzheimer disease. *Nat Rev Neurol* **6:** 99–107

Extance A (2010) Alzheimer's failure raises questions about disease-modifying strategies. *Nat Rev Drug Discov* **9:** 749–751

Fuwa H, Takahashi Y, Konno Y, Watanabe N, Miyashita H, Sasaki M, Natsugari H, Kan T, Fukuyama T, Tomita T, Iwatsubo T (2007) Divergent synthesis of multifunctional molecular probes to elucidate the enzyme specificity of dipeptidic γ-secretase inhibitors. *ACS Chem Biol* **2:** 408–418

Green RC, Schneider LS, Amato DA, Beelen AP, Wilcock G, Swabb EA, Zavitz KH (2009) Effect of tarenflurbil on cognitive decline and activities of daily living in patients with mild Alzheimer disease: a randomized controlled trial. *JAMA* **302:** 2557–2564

Hayashi I, Urano Y, Fukuda R, Isoo N, Kodama T, Hamakubo T, Tomita T, Iwatsubo T (2004) Selective reconstitution and recovery of functional γ-secretase complex on budded baculovirus particles. *J Biol Chem* **279:** 38040–38046

Herreman A, Serneels L, Annaert W, Collen D, Schoonjans L, De Strooper B (2000) Total inactivation of γ-secretase activity in presenilin-deficient embryonic stem cells. *Nat Cell Biol* **2:** 461–462

Hofmann K, Kiso Y (1976) An approach to the targeted attachment of peptides and proteins to solid supports. *Proc Natl Acad Sci USA* **73:** 3516–3518

Holtzman DM, Morris JC, Goate AM (2011) Alzheimer's disease: the challenge of the second century. *Sci Transl Med* **3:** 77sr71

Imamura Y, Watanabe N, Umezawa N, Iwatsubo T, Kato N, Tomita T, Higuchi T (2009) Inhibition of γ-secretase activity by helical β-peptide foldamers. *J Am Chem Soc* **131:** 7353–7359

Isoo N, Sato C, Miyashita H, Shinohara M, Takasugi N, Morohashi Y, Tsuji S, Tomita T, Iwatsubo T (2007) Aβ42 overproduction associated with structural changes in the catalytic pore of γ-secretase: common effects of Pen-2 N-terminal elongation and fenofibrate. *J Biol Chem* **282:** 12388–12396

Iwatsubo T, Odaka A, Suzuki N, Mizusawa H, Nukina N, Ihara Y (1994) Visualization of Aβ42(43) and Aβ40 in senile plaques with end-specific A beta monoclonals: evidence that an initially deposited species is Aβ42(43). *Neuron* **13:** 45–53

Kakuda N, Funamoto S, Yagishita S, Takami M, Osawa S, Dohmae N, Ihara Y (2006) Equimolar production of amyloid beta-protein and amyloid precursor protein intracellular domain from β-carboxyl-terminal fragment by γ-secretase. *J Biol Chem* **281:** 14776–14786

Kitamura T, Koshino Y, Shibata F, Oki T, Nakajima H, Nosaka T, Kumagai H (2003) Retrovirus-mediated gene transfer and expression cloning: powerful tools in functional genomics. *Exp Hematol* **31:** 1007–1014

Kopan R, Schroeter EH, Weintraub H, Nye JS (1996) Signal transduction by activated mNotch: importance of proteolytic processing and its regulation by the extracellular domain. *Proc Natl Acad Sci USA* **93:** 1683–1688

Kounnas MZ, Danks AM, Cheng S, Tyree C, Ackerman E, Zhang X, Ahn K, Nguyen P, Comer D, Mao L, Yu C, Pleynet D, Digregorio PJ, Velicelebi G, Stauderman KA, Comer WT, Mobley WC, Li YM, Sisodia SS, Tanzi RE *et al* (2010) Modulation of γ-secretase reduces β-amyloid deposition in a transgenic mouse model of Alzheimer's disease. *Neuron* **67:** 769–780

Kukar TL, Ladd TB, Bann MA, Fraering PC, Narlawar R, Maharvi GM, Healy B, Chapman R, Welzel AT, Price RW, Moore B, Rangachari V, Cusack B, Eriksen J, Jansen-West K, Verbeeck C, Yager D, Eckman C, Ye W, Sagi S *et al* (2008) Substrate-targeting {gamma}-secretase modulators. *Nature* **453:** 925–929

Li YM, Xu M, Lai MT, Huang Q, Castro JL, DiMuzio-Mower J, Harrison T, Lellis C, Nadin A, Neduvelil JG, Register RB, Sardana MK, Shearman MS, Smith AL, Shi XP, Yin KC, Shafer JA, Gardell SJ (2000) Photoactivated γ-secretase inhibitors directed to the active site covalently label presenilin 1. *Nature* **405:** 689–694

Lleo A, Berezovska O, Herl L, Raju S, Deng A, Bacskai BJ, Frosch MP, Irizarry M, Hyman BT (2004) Nonsteroidal anti-inflammatory drugs lower Aβ42 and change presenilin 1 conformation. *Nat Med* **10:** 1065–1066

Morohashi Y, Kan T, Tominari Y, Fuwa H, Okamura Y, Watanabe N, Sato C, Natsugari H, Fukuyama T, Iwatsubo T, Tomita T (2006) C-terminal fragment of presenilin is the molecular target of a dipeptidic γ-secretase-specific inhibitor DAPT (*N*-[*N*-(3,5-difluorophenacetyl)-*L*-alanyl]-*S*-phenylglycine *t*-butyl ester). *J Biol Chem* **281:** 14670–14676

Ogura T, Mio K, Hayashi I, Miyashita H, Fukuda R, Kopan R, Kodama T, Hamakubo T, Iwatsubo T, Tomita T, Sato C (2006) Three-dimensional structure of the γ-secretase complex. *Biochem Biophys Res Commun* **343:** 525–534

Okochi M, Fukumori A, Jiang J, Itoh N, Kimura R, Steiner H, Haass C, Tagami S, Takeda M (2006) Secretion of the Notch-1 Aβ-like peptide during Notch signaling. *J Biol Chem* **281:** 7890–7898

Osawa S, Funamoto S, Nobuhara M, Wada-Kakuda S, Shimojo M, Yagishita S, Ihara Y (2008) Phosphoinositides suppress γ-secretase in both the detergent-soluble and -insoluble states. *J Biol Chem* **283:** 19283–19292

Page RM, Baumann K, Tomioka M, Perez-Revuelta BI, Fukumori A, Jacobsen H, Flohr A, Luebbers T, Ozmen L, Steiner H, Haass C (2008) Generation of Aβ38 and Aβ42 is independently and differentially affected by familial Alzheimer disease-associated presenilin mutations and γ-secretase modulation. *J Biol Chem* **283:** 677–683

Page RM, Gutsmiedl A, Fukumori A, Winkler E, Haass C, Steiner H (2010) β-amyloid precursor protein mutants respond to γ-secretase modulators. *J Biol Chem* **285:** 17798–17810

Qi-Takahara Y, Morishima-Kawashima M, Tanimura Y, Dolios G, Hirotani N, Horikoshi Y, Kametani F, Maeda M, Saido TC, Wang R, Ihara Y (2005) Longer forms of amyloid beta protein: implications for the mechanism of intramembrane cleavage by γ-secretase. *J Neurosci* **25:** 436–445

Richter L, Munter LM, Ness J, Hildebrand PW, Dasari M, Unterreitmeier S, Bulic B, Beyermann M, Gust R, Reif B, Weggen S, Langosch D, Multhaup G (2010) Amyloid β 42 peptide (Aβ42)-lowering compounds directly bind to Aβ and interfere with amyloid precursor protein (APP) transmembrane dimerization. *Proc Natl Acad Sci USA* **107:** 14597–14602

Sato C, Morohashi Y, Tomita T, Iwatsubo T (2006) Structure of the catalytic pore of γ-secretase probed by the accessibility of substituted cysteines. *J Neurosci* **26:** 12081–12088

Sato C, Takagi S, Tomita T, Iwatsubo T (2008) The C-terminal PAL motif and transmembrane domain 9 of presenilin 1 are involved in the formation of the catalytic pore of the γ-secretase. *J Neurosci* **28:** 6264–6271

Sato T, Nyborg AC, Iwata N, Diehl TS, Saido TC, Golde TE, Wolfe MS (2006) Signal peptide peptidase: biochemical properties and modulation by nonsteroidal antiinflammatory drugs. *Biochemistry* **45:** 8649–8656

Takagi S, Tominaga A, Sato C, Tomita T, Iwatsubo T (2010) Participation of transmembrane domain 1 of presenilin 1 in the catalytic pore structure of the γ-secretase. *J Neurosci* **30:** 15943–15950

Takahashi Y, Hayashi I, Tominari Y, Rikimaru K, Morohashi Y, Kan T, Natsugari H, Fukuyama T, Tomita T, Iwatsubo T (2003) Sulindac sulfide is a noncompetitive γ-secretase inhibitor that preferentially reduces Aβ42 generation. *J Biol Chem* **278:** 18664–18670

Takami M, Nagashima Y, Sano Y, Ishihara S, Morishima-Kawashima M, Funamoto S, Ihara Y (2009) γ-Secretase: successive tripeptide and tetrapeptide release from the transmembrane domain of β-carboxyl terminal fragment. *J Neurosci* **29:** 13042–13052

Takasugi N, Tomita T, Hayashi I, Tsuruoka M, Niimura M, Takahashi Y, Thinakaran G, Iwatsubo T (2003) The role of presenilin cofactors in the γ-secretase complex. *Nature* **422:** 438–441

Tomita T, Maruyama K, Saido TC, Kume H, Shinozaki K, Tokuhiro S, Capell A, Walter J, Grunberg J, Haass C, Iwatsubo T, Obata K (1997) The presenilin 2 mutation (N141I) linked to familial Alzheimer disease (Volga German families) increases the secretion of amyloid β protein ending at the 42nd (or 43rd) residue. *Proc Natl Acad Sci USA* **94:** 2025–2030

Tomita T (2009) Secretase inhibitors and modulators for Alzheimer's disease treatment. *Expert Rev Neurother* **9:** 661–679

Tomita T, Takikawa R, Koyama A, Morohashi Y, Takasugi N, Saido TC, Maruyama K, Iwatsubo T (1999) C terminus of presenilin is required for overproduction of amyloidogenic Aβ42 through stabilization and endoproteolysis of presenilin. *J Neurosci* **19:** 10627–10634

Uemura K, Farner KC, Hashimoto T, Nasser-Ghodsi N, Wolfe MS, Koo EH, Hyman BT, Berezovska O (2010) Substrate docking to γ-secretase allows access of γ-secretase modulators to an allosteric site. *Nat Commun* **1:** 130

Uemura K, Lill CM, Li X, Peters JA, Ivanov A, Fan Z, DeStrooper B, Bacskai BJ, Hyman BT, Berezovska O (2009) Allosteric modulation of PS1/γ-secretase conformation correlates with amyloid β(42/40) ratio. *PLoS One* **4:** e7893

Watanabe N, Takagi S, Tominaga A, Tomita T, Iwatsubo T (2010) Functional analysis of the transmembrane domains of presenilin 1: participation of transmembrane domains 2 and 6 in the formation of initial substrate-binding site of gamma-secretase. *J Biol Chem* **285:** 19738–19746

Watanabe N, Tomita T, Sato C, Kitamura T, Morohashi Y, Iwatsubo T (2005) Pen-2 is incorporated into the γ-secretase complex through binding to transmembrane domain 4 of presenilin 1. *J Biol Chem* **280:** 41967–41975

Weggen S, Eriksen JL, Das P, Sagi SA, Wang R, Pietrzik CU, Findlay KA, Smith TE, Murphy MP, Bulter T, Kang DE, Marquez-Sterling N, Golde TE, Koo EH (2001) A subset of NSAIDs lower amyloidogenic Aβ42 independently of cyclooxygenase activity. *Nature* **414:** 212–216

THE JOURNAL OF BIOLOGICAL CHEMISTRY VOL. 286, NO. 29, pp. 26188–26197, July 22, 2011

Three-dimensional Structure of the Signal Peptide Peptidase*[S]

Received for publication, May 13, 2011 Published, JBC Papers in Press, June 2, 2011, DOI 10.1074/jbc.M111.260273

Hiroyuki Miyashita (宮下紘幸)[‡1,2], Yuusuke Maruyama (丸山雄介)[§1], Hayato Isshiki (一色隼人)[‡2], Satoko Osawa (大沢智子)[‡], Toshihiko Ogura (小椋俊彦)[§], Kazuhiro Mio (三尾和弘)[§], Chikara Sato (佐藤主税)[§3], Taisuke Tomita (富田泰輔)[‡¶4], and Takeshi Iwatsubo (岩坪威)[‡¶‖]

From the [‡]Department of Neuropathology and Neuroscience, Graduate School of Pharmaceutical Sciences, The University of Tokyo, Tokyo 113-0033, the [§]Biomedical Research Institute and Biomedicinal Information Research Center, National Institute of Advanced Industrial Science and Technology, Ibaraki 305-8561, the [¶]Core Research for Evolutional Science and Technology, Japan Science and Technology Agency, Tokyo 113-0033, and the [‖]Department of Neuropathology, Graduate School of Medicine, The University of Tokyo, Tokyo 113-0033, Japan

Signal peptide peptidase (SPP) is an atypical aspartic protease that hydrolyzes peptide bonds within the transmembrane domain of substrates and is implicated in several biological and pathological functions. Here, we analyzed the structure of human SPP by electron microscopy and reconstructed the three-dimensional structure at a resolution of 22 Å. Enzymatically active SPP forms a slender, bullet-shaped homotetramer with dimensions of 85 × 85 × 130 Å. The SPP complex has four concaves on the rhombus-like sides, connected to a large chamber inside the molecule. Intriguingly, the N-terminal region of SPP is sufficient for the tetrameric assembly. Moreover, overexpression of the N-terminal region inhibited the formation of the endogenous SPP tetramer and the proteolytic activity within cells. These data suggest that the homotetramer is the functional unit of SPP and that its N-terminal region, which works as the structural scaffold, has a novel modulatory function for the intramembrane-cleaving activity of SPP.

The intramembrane-cleaving proteases (I-CLiPs)[5] that sever the transmembrane domains of their substrates have been identified in a range of organisms and play a variety of roles in biological and pathological conditions (1). I-CLiPs have been classified into three groups: serine-, aspartyl-, and metalloprotease-type, according to the structure of active sites. Presenilin (PS) and signal peptide peptidase (SPP) family proteins belong to the group of aspartyl I-CLiPs (2, 3). These polytopic proteases have nine transmembrane domains with the two catalytic aspartates as YD and G*X*GD motifs. Several γ-secretase inhibitors cross-inhibit the SPP activity, suggesting that PS, the catalytic subunit of γ-secretase, and SPP share a similar structure and proteolytic mechanism (4–8). However, γ-secretase requires three cofactor proteins (*i.e.* nicastrin, aph-1, and pen-2) in addition to PS (9–11), whereas SPP alone exhibits catalytic function not requiring other protein cofactors (4). SPP is implicated in the clearance of signal peptides as well as misfolded membrane proteins (12–14). Moreover, some endoproteolytic products generated by SPP cleavage directly mediate signal transduction (15, 16). In fact, loss-of-function studies of SPP in model animals resulted in severe developmental defects, inferring a vital role of SPP in metazoan development (17–19). Furthermore, a growing body of evidence indicates that SPP activity plays an important role in the maturation of several pathogens including the hepatitis C virus and the malaria parasite (7, 20). Thus, understanding the structure and function relationship of SPP as well as the rational development of its inhibitors should have a significant therapeutic potential for these infectious diseases. Here, we found that SPP proteins formed a tetramer in the enzymatically active condition. Single particle reconstruction from electron microscopic images revealed that the purified SPP forms a bullet-like shape with concaves on the surface and a large chamber in the center. Intriguingly, overexpression of the N-terminal region of SPP, which is sufficient for the tetrameric assembly, led to the inhibition of the proteolytic activity. Our first study on the structure of SPP reveals its submolecular configuration and highlights a novel modulatory mechanism of the N-terminal region on the proteolytic activity of SPP.

EXPERIMENTAL PROCEDURES

Antibodies and Compounds—Rabbit polyclonal antibodies dSPPN1 and dSPPC1 were raised against glutathione *S*-transferase fused to amino acids 1–20 and 370–389 of *Drosophila* SPP (dSPP), respectively. Rabbit polyclonal antibody anti-

* This work is supported in part by grants-in-aid for young scientists (S) (to T. T.) from the Japan Society for the Promotion of Science (JSPS), by grants from the Strategic Japanese-Swiss Cooperative Program of the JST (to C. S.), by a grant-in-aid for scientific research on innovative areas, structural basis of cell-signaling complexes mediating signal perception, transduction and responses of a Ministry of Education, Culture, Sports, Science, and Technology (MEXT) (to C. S.), by the Targeted Proteins Research Program of the Japan Science and Technology Corporation (JST) (to T. T., T. I., C. S.), and by the Core Research for Evolutional Science and Technology of JST (to T. T. and T. I.), Japan.

[S] The on-line version of this article (available at http://www.jbc.org) contains supplemental Figs. S1–S4.

[1] Both authors contributed equally to this work.
[2] Research fellows of the JSPS.
[3] To whom correspondence should be addressed. Tel.: 81-29-861-5562; Fax: 81-29-861-6478; E-mail: ti-sato@aist.go.jp.
[4] To whom correspondence should be addressed: Dept. of Neuropathology and Neuroscience, Graduate School of Pharmaceutical Sciences, The University of Tokyo, 7-3-1 Hongo, Bunkyo-ku, Tokyo 113-0033, Japan. Tel: 81-3-5841-4868; Fax: 81-3-5841-4708 E-mail: taisuke@mol.f.u-tokyo.ac.jp.

[5] The abbreviations used are: I-CLiP, intramembrane-cleaving protease; DDM, *n*-dodecyl-β-D-maltopyranoside; PS, presenilin; SPP, signal peptide peptidase; dSPP, *Drosophila* SPP; 3FSPP, 3×FLAG-tagged human SPP; ERSE, endoplasmic reticulum stress response element; NT, N terminus; BN-PAGE, Blue-Native PAGE; SEC, size-exclusion gel chromatography.